Discovery of pyrazole derivatives as cellular active inhibitors of histone lysine specific demethylase 5B (KDM5B/JARID1B)

Bing Zhao, Qianqian Liang, Hongmei Ren, Xinhui Zhang, Yang Wu, Kun Zhang, Li-Ying Ma, Yi-Chao Zheng, Hong-Min Liu

PII: S0223-5234(20)30128-8

DOI: https://doi.org/10.1016/j.ejmech.2020.112161

Reference: EJMECH 112161

To appear in: *European Journal of Medicinal Chemistry*

Received Date: 21 December 2019

Revised Date: 15 February 2020

Accepted Date: 18 February 2020

Please cite this article as: B. Zhao, Q. Liang, H. Ren, X. Zhang, Y. Wu, K. Zhang, L.-Y. Ma, Y.-C. Zheng, H.-M. Liu, Discovery of pyrazole derivatives as cellular active inhibitors of histone lysine specific demethylase 5B (KDM5B/JARID1B), *European Journal of Medicinal Chemistry* (2020), doi: https://doi.org/10.1016/j.ejmech.2020.112161.

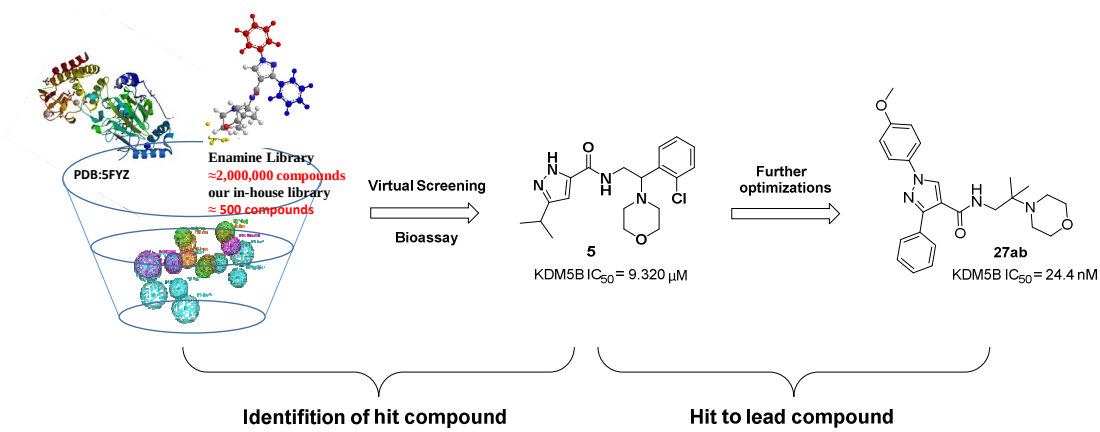

Discovery of pyrazole derivatives as cellular active inhibitors of histone lysine specific demethylase 5B (KDM5B/JARID1B)

*Bing Zhao[1, #], Qianqian Liang[1, #], Hongmei Ren [1, #], Xinhui Zhang[1], Yang Wu[1], Kun Zhang[1], Li-Ying Ma[1, *], Yi-Chao Zheng [1, *] and Hong-Min Liu [1, *]*

[1]*Collaborative Innovation Center of New Drug Research and Safety Evaluation, Henan Province; Key Laboratory of Technology of Drug Preparation (Zhengzhou University), Ministry of Education of China; Key Laboratory of Henan Province for Drug Quality and Evaluation; Institute of Pharmaceutical research and School of Pharmaceutical Sciences, Zhengzhou University, Zhengzhou 450001, PR China*

ABSTRACT: KDM5B (also known as PLU-1 and JARID1B) is 2-oxoglutarate and Fe^{2+} dependent oxygenase that acts as a histone H3K4 demethylase, which is a key participant in inhibiting the expression of tumor suppressors as a drug target. Here, we present the discovery of pyrazole derivatives compound **5** by structure-based virtual screening and biochemical screening with IC_{50} of 9.320μM against KDM5B, and its subsequent optimization to give 1-(4-methoxyphenyl)-N-(2-methyl-2-morpholinopropyl)-3-phenyl-1H-pyrazole-4-carboxamide (**27ab**), a potent KDM5B inhibitor with IC_{50} of 0.0244μM. In MKN45 cells, compound **27ab** can bind and stabilize KDM5B and induce the accumulation of H3K4me2/3, bona fide substrates of KDM5B, while keep the amount of H3K4me1, H3K9me2/3 and H3K27me2 without change. Further biological study also indicated that compound **27ab** is a potent cellular active KDM5B inhibitor that can inhibit MKN45 cell proliferation, wound healing and migration. In sum, our finding gives a novel structure for the discovery of

KDM5B inhibitor and targeting KDM5B may be a new therapeutic strategy for gastric cancer treatment.

INTRODUCTION

To data, some studies indicate that the occurrence and development of cancer are closely related to epigenetics, including DNA and RNA modification, histone modification and non-coding RNAs [1-5]. Among the diverse epigenetic mechanisms that modify chromatin structure to regulate gene expression, histone modification plays a significant role in gene transcription, genomic integrity and chromosome stability [6-9]. Until now, two classes of lysine demethylases can remove methyl groups from lysine residues: one is Histone lysine demethylase 1 (KDM1) subfamily, the other is Histone lysine demethylase 2-7 (KDM2-KDM7) subfamily which contain JmjC domain. KDM1 subfamily is flavin adenine dinucleotide (FAD) dependent oxygenase and KDM2-7 subfamily is α-ketoglutarate (2-OG) /Fe^{2+} - dependent oxygenase [10-12]. Of the JmjC containing KDMs, lysine demethylase 5B (KDM5B) is a lysine demethylase that can erase methyl group from H3K4me1/2/3 [13], and it is overexpressed and plays a vital role in diverse cancers [14, 15], such as breast cancer [16-18], gastric cancer [19-22], hepatocellular carcinoma [23], and lung cancer [24, 25]. Hence, targeting KDM5B is a new therapeutic strategy for cancer treatment [26, 27], and a range of small-molecule inhibitors of KDM5B has been reported, the majority of which are 2-OG competitive and coordinate to Fe^{2+} in the catalytic site, for example compounds **1-4** [28-31] (Figure 1). Although several KDM5B inhibitors have been developed, there is still no KDM5B inhibitors in clinic trials due to their cell permeability, specificity and potency and so on. Hence, it is still a challenging subject to develop potent KDM5B inhibitors to abrogate the abnormal overexpression and activation of KDM5B.

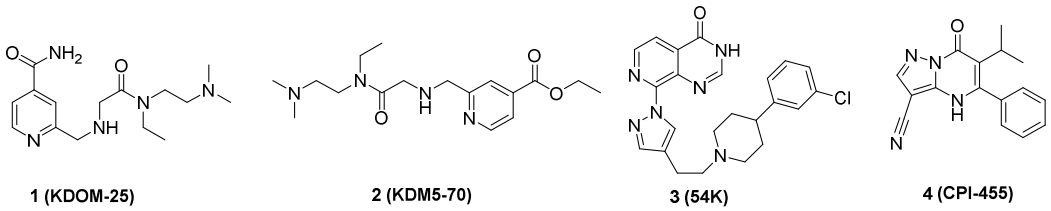

Figure 1. Reported small molecule inhibitors of KDM5B.

High-throughput virtual screening (HTVS) is a powerful and efficient tool for drug discovery [32-34]. In order to discover novel KDM5B inhibitor with new scaffold, HTVS was performed to identify hit compound using known receptor structure (PDB code: 5FYZ, resolution: 1.75 Å). Over 2 million compounds from the database Enamine and our in-house compound library (approximate 500 compounds) were screened, and hit compound **5** (IC_{50} = 9.320 μM) was found. Moreover, through subsequent structural based optimization, compound **27ab** was developed as a potent KDM5B inhibitor with IC_{50} = 0.0244 μM, which improves the potency for more than 382-fold, comparing to the hit compound **5**.

Herein, we described the identification of pyrazole derivatives as KDM5B inhibitors with the aid of HTVS and the subsequent structure-based optimization. Among our synthesized compounds, compound **27ab** (IC_{50} = 0.0244 μM) is a potent and cellular active KDM5B inhibitor (Figure 2) that can induce the accumulation of H3K4me2/3 as a chemical tool. Besides, compound **27ab** can also inhibit the proliferation, colony formation and would healing of gastric cancer cell line MKN45. Our finding gives a novel structure for the discovery of KDM5B inhibitor and targeting KDM5B may be a new therapeutic strategy for gastric cancer treatment.

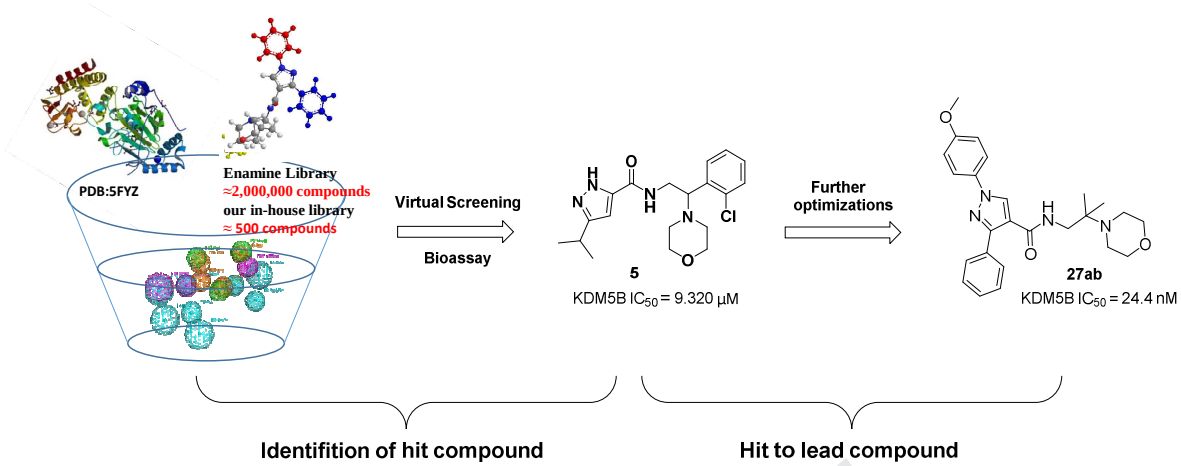

Figure 2. Identification of hit compound **5** from virtual screening and subsequent optimizations gives compound **27ab**

RESULTS AND DISCUSSION

2.1. The general routes

The general routes of the designed compounds were depicted in Scheme 1-4. In this work, the pyrazole scaffold was also replaced with pyridine and triazole. The compounds **13a-b** and **14a-b** of general routes are presented in Scheme 1. Treatment of ketones **6** with tert-butyl hydrazinecarboxylate **7** in EtOH gave compounds **8a-b**, which then reacted with $POCl_3$ in DMF [35, 36], affording compounds **9a-b** [37]. Oxidization of **9a-b** using $KMnO_4$ yielded **10a-b**. Compounds **13a-b and 14a-b** were prepared via reaction of compound **10a-b** and commercial compounds **11a-b** with appropriately 2-morpholinoethan-1-amine **12**.

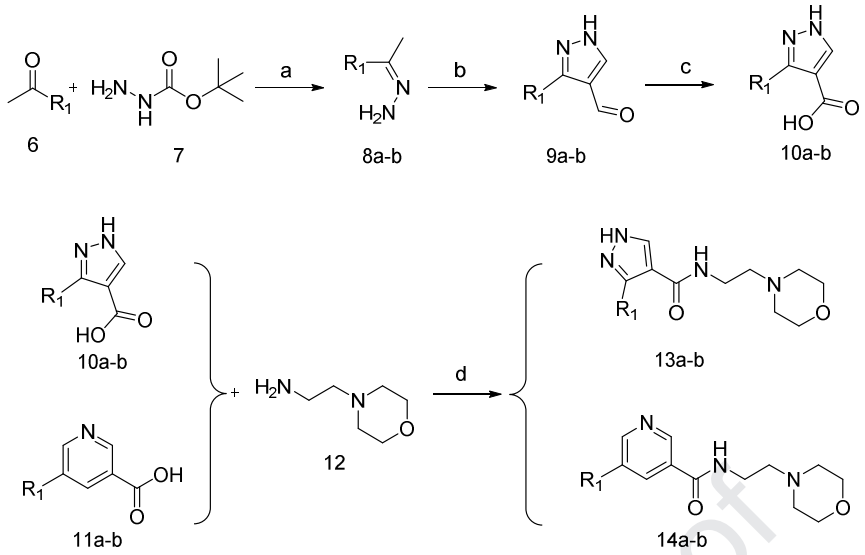

Scheme 1. Synthesis route of compounds **13a-b and 14a-b**. Reaction conditions: a) cat. AcOH, EtOH, reflux, 4h/TFA, DCM, 0.5h; b) $POCl_3$, DMF; c) $KMnO_4$, KOH; d) EDCI, HOBT, DCM, rt, 1h.

As shown in Scheme 2, the **16** were prepared via prolonged heating of kinds of ketones **6** and phenylhydrazines with different substituents **15**. Treatment of compounds **16** with $POCl_3$ in DMF, affording compounds **17**, which then reacted with KMnO4 in dioxane and water to yield the key intermediate derviatives**18**. In addition, as shown in Scheme 3, compounds **23 and 25** were prepared via reaction of morpholine **21** and trimethylsilanecarbonitrile **22** wizth appropriately acetone **19**, cyclohexanone **20**, respectively. Treatment of compounds **23** and **25** with $LiAlH_4$ in THF gave compounds **24** and **26**. Compounds **18a-r** were modified by reacting with compound **24, 26** and kinds of amines, respectively, affording compounds **27a-ac**.

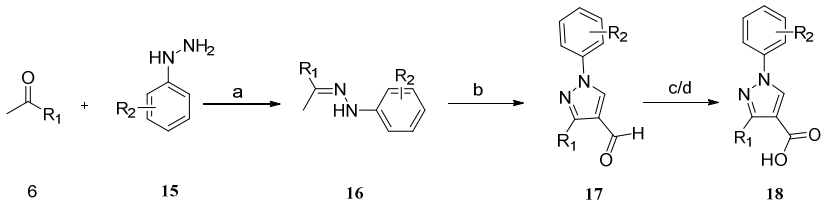

Compd.	R_1	R_2	Compd.	R_1	R_2
18a		H	18j		p-CH_3
18b	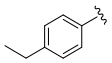	H	18k		o-CH_3
18c	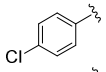	H	18l		m-CH_3
18d	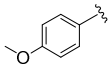	H	18m		p-CH_2CH_3
18e		H	18n		p-$CH(CH_3)_2$
18f		H	18o		p-OCH_3
18g	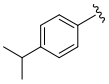	H	18p		o-OCH_3
18h		H	18q		p-Cl
18i		H	18r		p-CH_3

Scheme 2. Synthesis route of intermediattes**18a-r**. Reaction conditions: a) cat.AcOH, EtOH, reflux; b) $POCl_3$, DMF; c) $KMnO_4$, KOH; d) 1, 4-dioxane/H_2O, rt, 12h;

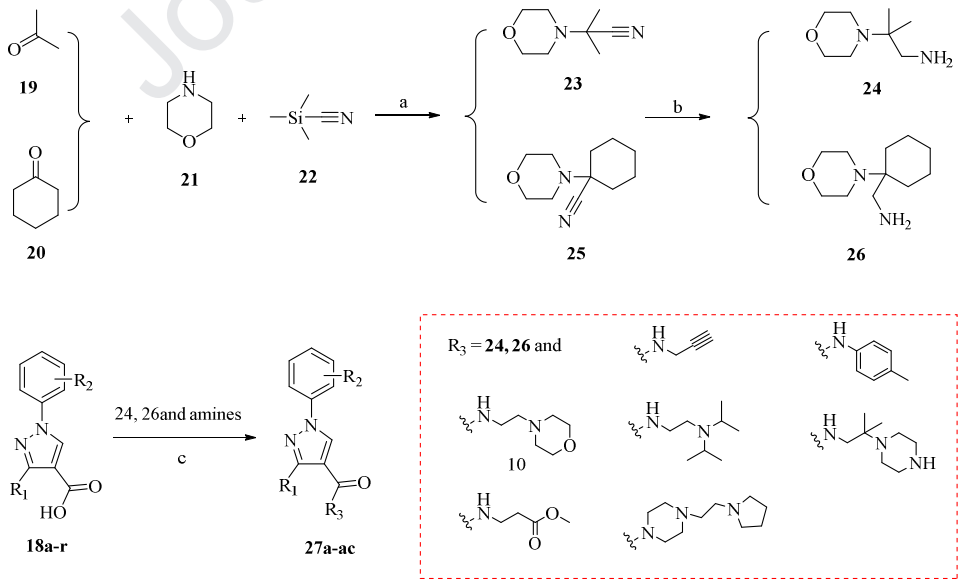

Scheme 3. Synthesis route of compounds **27a-c** and segments of amino. Reaction conditions: a) EtOH, reflux, 5h; b) THF, $LiAlH_4$, 0□, 6h; c) EDCI, HOBT, DCM, rt, 1h.

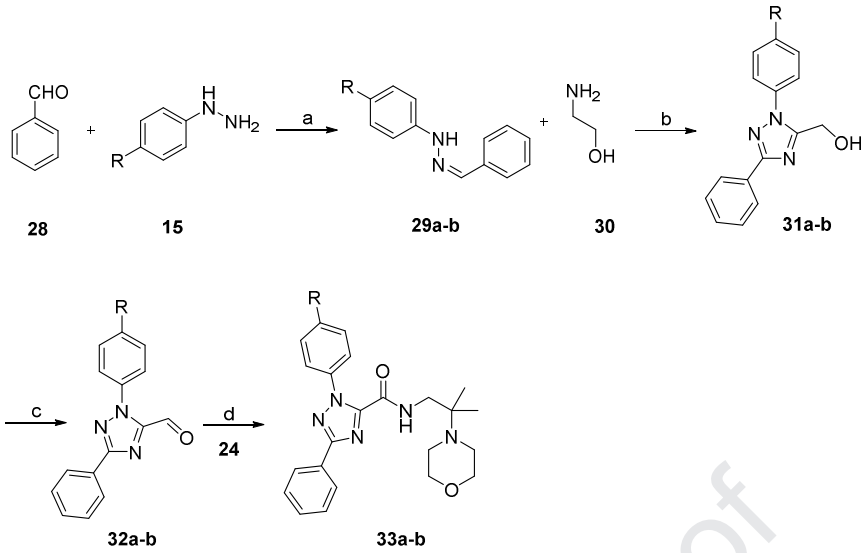

Scheme 4. Synthesis route of compounds **33a-b**. a) cat.AcOH, EtOH, reflux; b) cat.I_2, TBHP, MeCN, 90□; c) DCM, Dess-martin periodinane (DMP), 0□-rt; d) THF, t-BuOK, rt.

As shown in Scheme 4, treatment of benzaldehyde **28** with substituted phenylhydrazine **15** in EtOH gave compounds **29a-b**, which were allowed to react with ethanolamine **29a-b** via the iodine-catalyzed in MeCN to yield compounds **31a-b**. Treatment of compounds **31a-b** with DMP in DCM, affording compounds **32a-b** [38], which then reacted with 2-methyl-2-morpholinopropan-1-amine **24** in THF, under the presence of t-BuOK, to yield compounds **33a-b**.

2.2. Evaluation of biological activity

2.2.1. KDM5B inhibitory activity and SARs

All synthesized compounds were evaluated for their inhibitory activity against KDM5B using Amplified Luminescent Proximity Homogeneous Assay (ALPHA) and CPI-455 was used as the positive control [31, 39]. The inhibitory activity results of candidate compounds were shown in Table 1-4. The hit compound **5** identified from

the database Enamine was characterized to inhibit KDM5B with IC_{50} of 9.320 μM, which encouraged further structural optimization.

Firstly, simplified chiral amine fragments and replacement of the pyrazole ring in **5** with pyridine ring led to the formation of compounds **13a-b** and **14a-b** (Table 1). Clearly, compound **13a** and **14a-b** bearing pyridine ring, were found to be inactive toward KDM5B. Compound **13b** exhibited potent inhibitory activity with IC_{50} values of 5.390 μM toward KDM5B. This gave us more confidence of modelled binding of **5** to the KDM5B, albeit compound **14a-b** did not perform acceptable activity, which suggested the importance of pyrazole ring for KDM5B inhibitory activity.

Table 1. Inhibitory effect of compounds **13a-b** and **14a-b** on KDM5B.

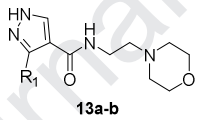

13a-b

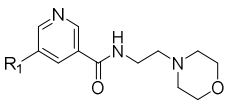

14a-b

Compd.	R1	Inhibition at 10 μM	IC_{50}/μM
13a	CH_3	21.53%	>10
13b		75.71%	5.390
14a	CH_3	33.65%	>10
14b		42.50%	>10
CPI-455	-	-	10.52 ± 0.23nM

As shown in Table 2, further structural modifications displayed that the identification of pyrzole and benzene ring containing compounds **27a,** which inactivated KDM5B potency (IC_{50} = 0.3102 μM), performed about 18-fold more potency than compound **13b**. In-depth structural optimizations focusing on replacement of R1 and R2 groups affiliated the pyrzole core were performed, yield compounds **27a-27o**. Most of them

showed improved KDM5B inhibitory activity. Compounds **27o** showed good activity with an IC_{50} value of 108.3nM, about 2-fold increase compared with compound **27a**. Compounds **27a-27h** contain the same phenyl group (R2), replacement of R1 group with furyl, pyridyl and phenyl groups with different substituents. At 10μM, the inhibitory effect of compounds **27g, 27h** was significantly decreased with less than 10% inhibition. The remaining compounds involving a hydrophobic R1 with substituents displayed comparable and potent efficacy towards KDM5B. Interestingly, modifications of R2 in compounds **27i-27o** were found to be inactive against KDM5B except compound **27o**. Conversely, when pyrazole scaffold with a larger substituted phenyl group, namely **27h** and **27n**, the inhibitory activity decreased significantly.

Table 2. Inhibitor effect of compounds **27a-o** on KDM5B.

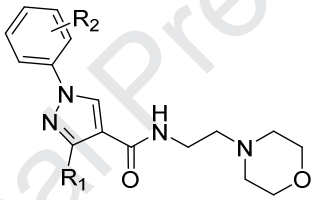

Compd.	R_1	R_2	Inhibition at 10μM	IC_{50} (μM)/IR
27a		H	76.42%	0.3102
27b		H	75.38%	0.3353
27c		H	81.26%	0.2371
27d	p-chlorophenyl	H	71.95%	0.5716
27e	p-methoxylphenyl	H	82.32%	0.2382
27f	p-ethylphenyl	H	45.32%	1.3506
27g	o-methylphenyl	H	9.25%	>10
27h	p-Isoproplphenyl	H	-5.81%	>10

27i	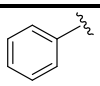	p-Cl	8.69%	>10
27j		p-CH_3	66.78%	0.8507
27k		o-CH_3	-7.78%	>10
27l		m-CH_3	20.92%	>10
27m		p-CH_2CH_3	20.03%	>10
27n		p-$CH(CH_3)_2$	14.81%	>10
27o		p-OCH_3	93.05%	0.1083
CPI-455	-			10.52 ± 0.23nM

Based on above findings, the third-round structural modification were primarily focused on variations of R3. Interestingly, compound **27v** inactivated KDM5B with IC_{50} of 73.0 nM, exhibited about 4.2-fold increase in potency, comparable to compound **27a** (IC_{50} = 310.2 nM, Table 2). 4-Methoxyl-benzyl-substituted compound **27ab** exhibited significantly increased potency against KDM5B with IC_{50} of 24.4nM, exhibited about 4.5-fold in potency, comparable to compound **27o** (IC_{50} = 108.3 nM, Table 2). The remaining compounds with different R3 were slightly more potent than compound **27a**, while they were not significantly increased. Compounds **27ac** bearing the 2-methoxy benzyl group, displayed acceptable potency at nanomolar levels (IC_{50} = 93.20 nM), but was less potent than compound **27ab**.

Table 3. Inhibitory effect of compounds **27p-ac** on KDM5B.

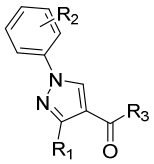

Compd.	R1	R2	R3	Inhibition at 10μM	IC50 (μM)/IR
27p		H	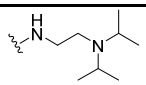	67.01%	2.2359
27q		H	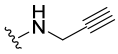	84.63%	0.3479
27r		H	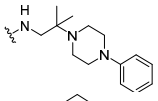	92.28%	0.2004
27s		H	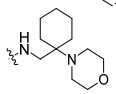	-1.95%	>10
27t		H	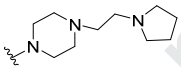	86.57%	0.2320
27u		p-OCH_3	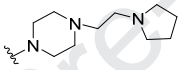	17.25%	>10
27v		p-CH_3	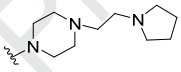	94.23%	0.0730
27w	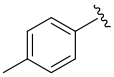	p-CH_3	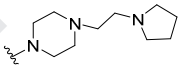	76.45%	0.8507
27x		p-CH_3	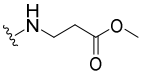	82.13%	0.2515
27y		p-CH_3	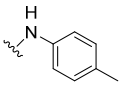	79.46%	0.3234
27z		p-CH_3	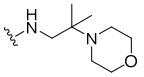	82.36%	0.1912
27aa		p-Cl	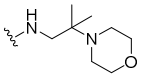	62.01%	0.5409
27ab		p-OCH_3	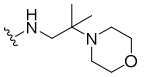	95.78%	0.0244
27ac		o-OCH_3	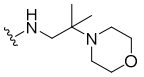	92.32%	0.0932
CPI-455	-				10.52 ± 0.23nM

Finally, the effects of the core scaffold toward KDM5B were explored by scaffold hopping strategy, and compounds **33a-b** were compared. According to the Table **4**,

the pyrazole scaffold was also replaced with triazole, leading to the generation of compounds **33a** and **33b**, which were found to be inactive toward KDM5B (IC_{50} > 10 μM), highlight the essential pyrazole scaffold for the activity.

Table 4. Activity of compounds **27ab** and **33a-b** on KDM5B.

Compd.	Structure	Inhibition at 10μM	IC_{50} (μM)
27ab	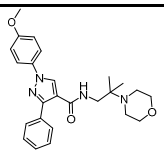	95.78%	0.0244
33a	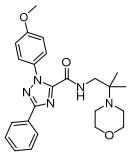	28.03%	>10
33b	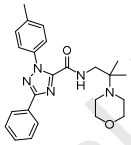	28.89%	>10
CPI-455	-		10.52 ± 0.23nM

As we have identified compound **27ab** as the most potent KDM5B inhibitor among our synthesized compounds (Figure 3A), selectivity of compound **27ab** against other KDMs was also performed and results showed that compound **27ab** may inhibit KDM4A for 5.12%, 29.36% and 56.25% at 0.01 μM, 0.25μM and 1 μM, respectively; KDM4C for 3.52%, 39.36% and 50.12% at 0.01 μM, 0.25μM and 1 μM, respectively; KDM5A for 20.12%, 62.36% and 79.32% at 0.01 μM, 0.25μM and 1 μM, respectively; KDM5C for 16.35%, 62.11% and 80.24% at 0.01 μM, 0.25μM and 1 μM, respectively and KDM6B for 3.57%, 12.37% and 19.57% at 0.01 μM, 0.25 μM and 1 μM, respectively (Figure 3B), while compound **27ab** may inhibit KDM4A with IC_{50} = 0.9542 ± 0.0231 μM, KDM4C with IC_{50} = 1.1125 ± 0.0301 μM, KDM5A with

IC_{50} = 0.0249 ± 0.0011 μM, KDM5C with IC_{50} = 0.0248 ± 0.0019 μM, and inhibit KDM6A with IC_{50} more than 1 μM. All these results suggested that compound **27ab** is a potent KDM5B inhibitor with acceptable selectivity against KDM5A/B/C, while it performed poor activity against KDM4A/C and KDM6B.

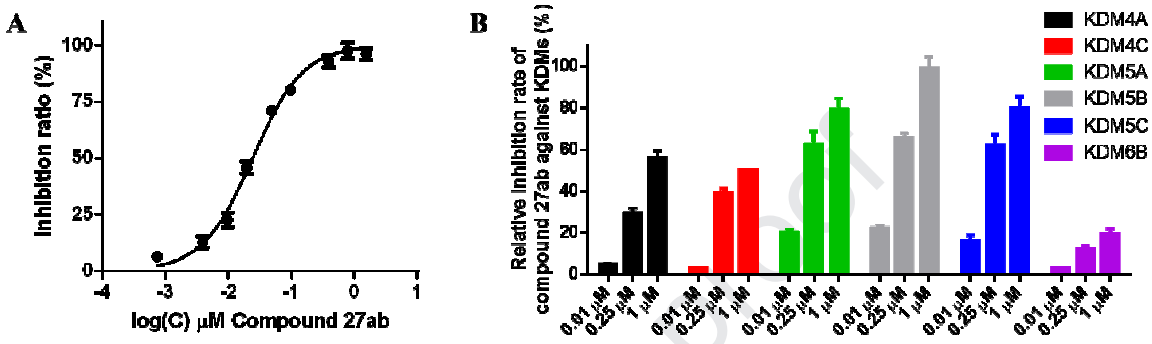

Figure 3. Inhibitory activity of compound **27ab** against KDMs. (A) Inhibitory curve of compound **27ab** against KDM5B; (B) Inhibition rate of compound **27ab** against KDM4A, KDM4C, KDM5A, KDM5B, KDM5C and KDM6B at 0.01 μM, 0.25 μM and 1 μM, respectively. The data represent the mean ± SD for three independent experiments.

2.3. Molecular docking studies

A molecular docking study was carried out to predict the binding mode of the studied compounds with KDM5B using Molecular Operating Environment (MOE) platform (v201608). KDM5B protein structure was extracted from Protein Data Bank with code 5FYZ (PDB code: 5FYZ, Resolution: 1.75 Å) and was prepared by adding hydrogen atoms, removing water molecules and small molecules ligand, the docking studies were in accordance with the results of KDM5B inhibitory activity, and gave more SAR information of pyrazole derivatives. The 2D binding modes of compound **27ab** with KDM5B were shown in Figure 4A. We characterized that compound **27ab**

fits well in the tight flat binding pocket of KDM5B, and the oxygen atom of morpholine has directly bind with the Mn ion, the distance was 2.1 Å (Figure 4A/4B). The phenyl with p-methoxyl group of compound **27ab** would be located in the junction of hydrophobic pocket and hydrophilic pocket, the phenyl was surrounding by Tyr 488, Tyr 425, and Val 489 (Figure 4A), and had π-π stacking with benzene ring of Tyr 488. Also, the oxygen atom of methoxyl formed hydrogen bond with Lys 517, the distance was 2.1 Å (Figure 4B). Addition, the nitrogen of acidamide had hydrogen interation with Tyr 488 and the distance was 2.9 Å.

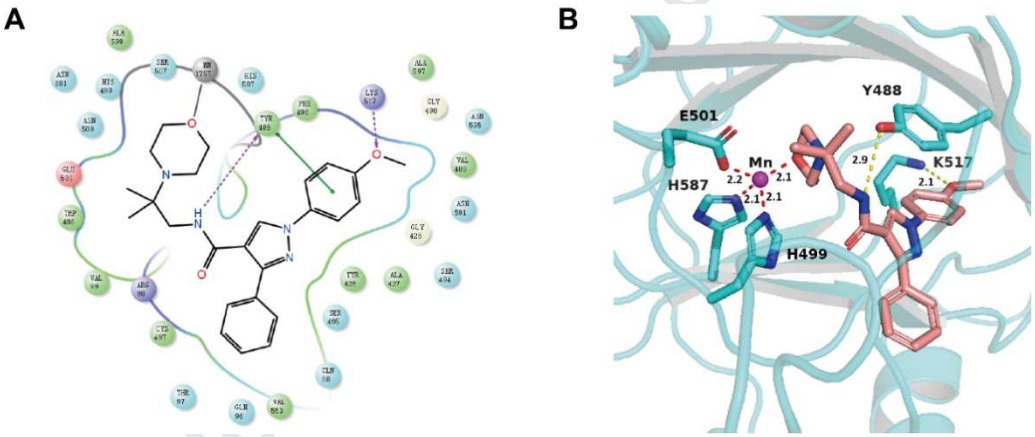

Figure 4. The molecular docking result of compound **27ab** in binding with KDM5B (PDB code: 5FYZ). (A) 2D results of compound **27ab** catalytic site of KDM5B; (B) 3D close-up views of hydrogen bond interactions between compound **27ab** and KDM5B; Binding pocket is indicated with transparent surface with compound **27ab** shown in brown and protein shown in cyan; Mn ion used as the crystallographic surrogate for the catalytic $Fe^{2+}$is shown as purple red sphere.

2.4. Compound 27ab is a target engaged KDM5B inhibitor in cells

As KDM5B was reported to be overexpressed in gastric cancer and is necessary for gastric cancer cell proliferation and metastasis [22, 26], and gastric cancer is the fifth

most common cancer in the world and the third most frequent cause of neoplasm-related deaths [22, 40]. Cellular activity of compound **27ab**, one of our most potent synthesized KDM5B inhibitors, was applied in gastric cancer cells. Before the cellular activity study of compound **27ab**, seven gastric cancer cells were collected and subjected to evaluate the KDM5B expression in these cells. As shown Figure 5A and 5B, expression of KDM5B in MKN45 cell line was the highest among all the tested gastric cancer cell lines. So, MKN45 was chosen for the following KDM5B inhibitor study.

As compound **33a** shares similar structure with compound **27ab**, but not active against KDM5B, hence, it was chosen as a negative control for some of the following studies. First, cellular thermal shift assay was employed to assess the cellular target engagement of compound **27ab** in MKN45 cells. As shown in Figure 5C & D, cellular KDM5B protein was denatured at 46 □ in MKN45 cells in the presence of different concentrations of compound **27ab** and compound **33a**. After 1h treatment of indicated compound, thermal stability of cellular KDM5B protein was investigated and results revealed that compound **27ab** can stabilize KDM5B in a dose dependent manner (Figure 5C), while the negative control compound **33a** failed to stabilize KDM5B in MKN45 cells (Figure 5D), all these results confirmed the cellular target engagement of compound **27ab** in MKN45 cells.

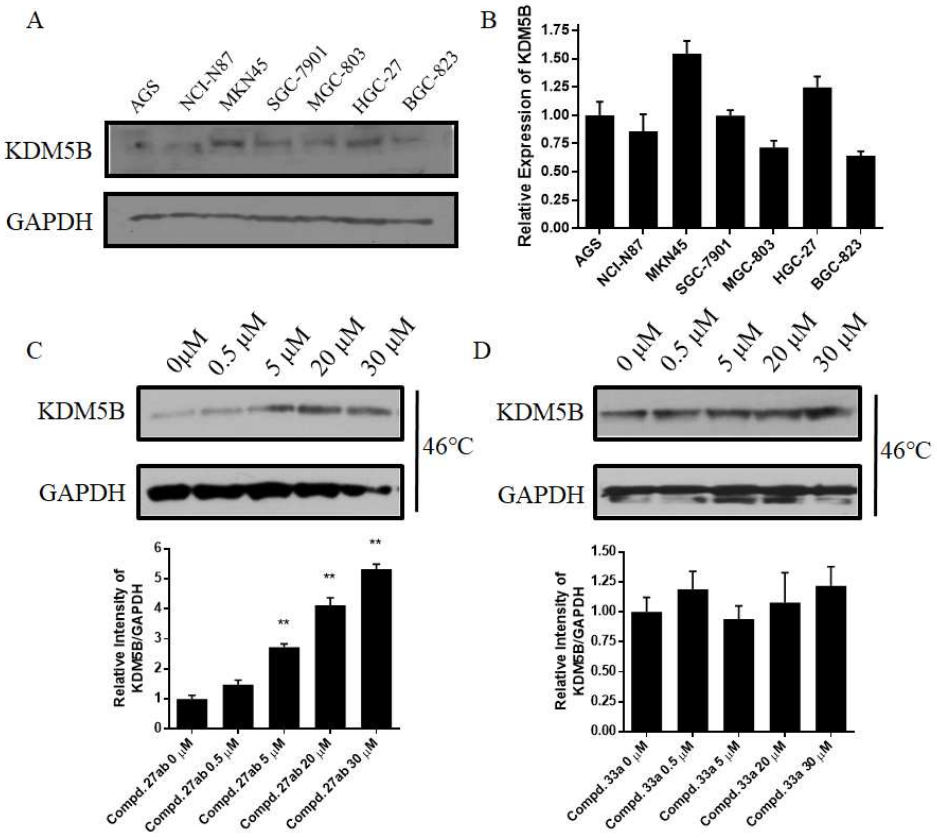

Figure 5. Cellular engagement of compound **27ab**. (A) Expression of KDM5B in gastric cancer cell lines AGS, NCI-N87, MKN45, SGC-7901, MGC-803, HGC-27 and BGC-823 were evaluated by Western Blotting, GAPDH was used as loading control; (B) Density quantification of KDM5B in the indicated gastric cancer cell lines; (C) Thermal stability of KDM5B in MKN45 cells treated with compound **27ab** for 1 h and then heated at 46 □ for 3 min; (D) Thermal stability of KDM5B in MKN45 cells treated with compound **33a** for 1 h and then heated at 46 □ for 3 min. GAPDH was used as a loading control. All experiments were repeated for three times.

2.5. Compound 27ab inactivates KDM5B in MKN45 Cells

As stated above, compound **27ab** is a target engagement KDM5B inhibitor in cells, hence, diverse substrates of methylated histone 3 were screened to evaluate its cellular activity and cellular selectivity. As shown in Figure 6A, 5 days treatment of compound **27ab**, from 0.5 μM to 20 μM, for MKN45 induced significant

accumulation of KDM5B substrate H3K4me2/3, while the negative compound **33a** failed to induce the accumulation of H3K4me2/3. Nevertheless, amount of H3K4me1 was kept constant in the presence of both compound **27ab** and compound **33a**. On the other hand, several substrates of KDM4 family and KDM6 family, including H3K9me2, H3K9me3 and H3K27me2, were also investigated to explore their accumulation with the compound treatment. Results in Figure 6A suggested that compound **27ab** failed to induce the expression of KDM4 family substrates H3K9me2 and H3K9me3, and so did the negative compound. Similarly, amount of H3K27me2, substrate of KDM6 family, was kept unchanged with the treatment of either compound **27ab** or the negative compound, even at high concentration as 20μM. To further confirm the KDM5B inhibitory effect of compound **27ab** *in situ*, immunofluorescence using H3K4me2/3 antibody with indicated treatment were performed with the aid of high content screening for quantification. As shown in Figure 6B-C, compound **27ab** induced the accumulation of H3K4me2 and H3K4me3 *in situ* in a dose dependent manner when it was applied to MKN45 cells for 5 days, while the negative compound **33a** induced hardly accumulation of H3K4me2 and H3K4me3. To sum up, compound **27ab** can inactivate KDM5B in MKN45 cells without significant impact on the activity of KDM4 and KDM6 families.

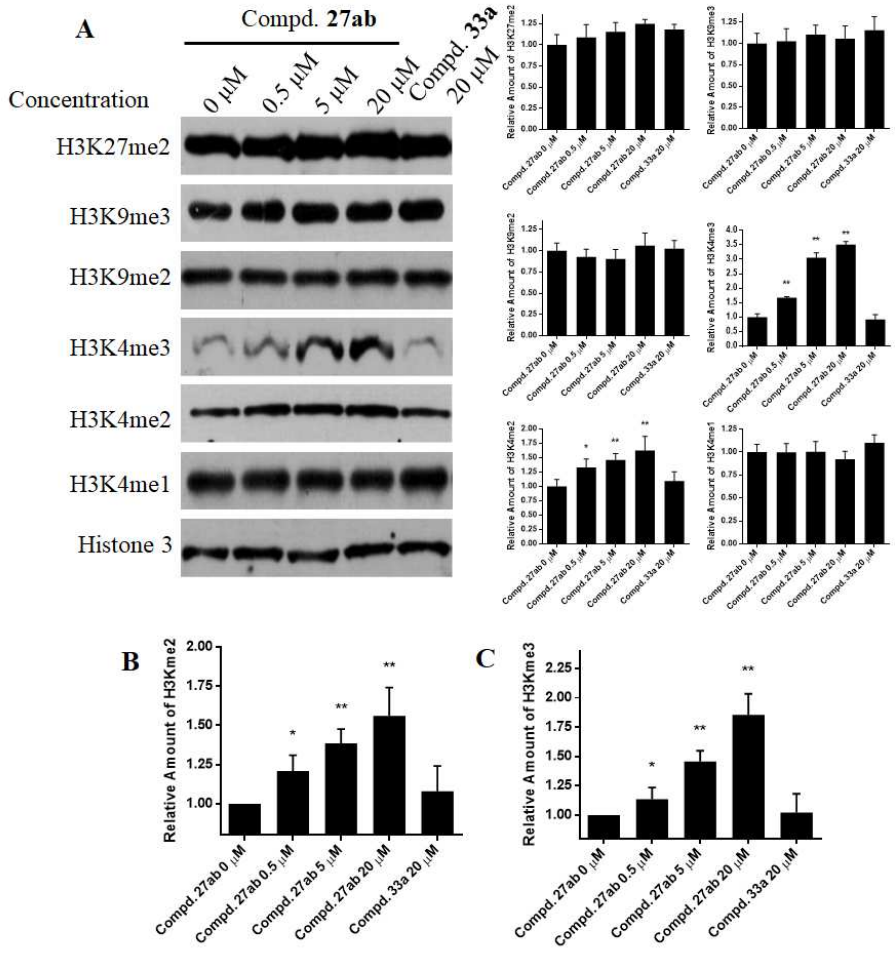

Figure 6. Compound **27ab** induced the accumulation of H3K4me2/3 in MKN45 cells. (A) Western Blotting analysis of the amount of H3K4me1/2/3, H3K9me1/2 and H3K27me2 in MKN45 cells with indicated treatment for 5 days; (B & C) High content analysis of H3K4me2 (B) and H3K4me2 (C) in MKN45 cells that were incubated with indicated compounds for 5 days. Compound **33a** was used as a negative control. Histone 3 was used as loading control. The data represent the mean ± SD for three independent experiments. *P < 0.05, **P < 0.01.

2.6. Compound 27ab inhibits MKN45 cells proliferation, wound healing and migration in a time and dose dependent manner in MKN45 cells

As KDM5B contributes to gastric cancer cell proliferation and metastasis [22, 26], we tried to investigate the biological role of compound **27ab** in gastric cancer cells. First,

antiproliferation activity of compound **27ab** was evaluated. After cells were treated for 4 days, both compound **27ab** and CPI-455 performed moderate antiproliferation activity in MKN45 cells with IC50 as 26.72 ± 2.28 μM and 30.33 ± 1.71 μM (Figure 7A), respectively. Meanwhile, 6 days treatment of compound **27ab** and CPI-455 inactivated the proliferation of MKN45 cells with IC50 as 20.56 ± 2.91 μM and 23.79 ± 1.09 μM (Figure 7B), respectively, but no antiproliferation effect against normal human gastric epithelial GES-1 cell line (antiproliferation rate < 10% even at 100 μM). On the other hand, compound **33a** inhibited 10.32% and 13.24% of the proliferation rate of MKN45 cells for 4 days and 6 days exposure, respectively, which means compound **33a** is inactive against MKN45 proliferation as a negative compound. As KDM5B was identified as a migration promoter in gastric cancer, further wound healing assay and transwell experiment were conducted. Results in Figure 7C suggests that compound **27ab** can inhibit the wound healing in a dose and time dependent manner, while the negative compound **33a** failed to inhibit the wound healing. In the 20 μM group, compound **27ab** showed equivalent activity as 20 μM CPI-455 in inhibiting the wound healing. Besides, activity of compound **27ab** against cell migration was investigated. As the transwell experiment showed in Figure 7D, different concentrations of compound **27ab** can suppress the migration of MKN45 cells in a concentration dependent manner for 24h treatment, and compound **27ab** inhibited cell migration more potently than CPI-455 at 20 μM, while the negative compound **33a** failed to inhibit cell migration even at 20 μM. In a nutshell, compound

27ab can inhibit MKN45 cell proliferation, would healing and migration by targeting KDM5B with similar potency as CPI-455.

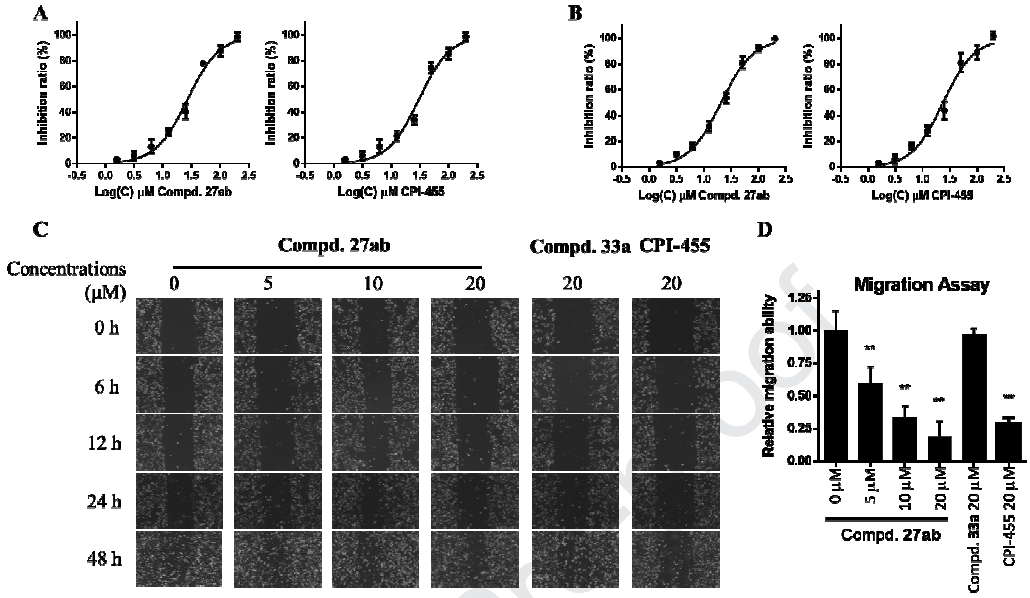

Figure 7. Compound **27ab** inhibited MKN45 cells proliferation and migration in a time and dose dependent manner. (A) Proliferation assay of compound **27ab** and CPI-455 in MKN45 cells for 4 days treatment; (B) Proliferation assay of compound **27ab** and CPI-455 in MKN45 cells for 6 days treatment; (C) Wound healing assay in MKN45 cells with indicated treatments at 0h, 6h, 12, 24h and 48h; (D) Migration assay was performed with transwell experiment with indicated treatments for 24h. Compound **33a** was used as a negative control, and CPI-455 was used as a positive control. All experiments were repeated for three times. The data represent the mean ± SD for three independent experiments. *P < 0.05, **P < 0.01.

3. Conclusions

In this study, the (R)-N-(2-(2-chlorophenyl)-2-morpholinoethyl)-3-isopropyl-1H-pyrazole-4-carboxamide (compound **5)** was firstly discovered as a KDM5B inhibitor based on HTVS and biochemical screening. Then, a series of pyrazole derivatives

were designed and synthesized through structural based optimization and obtained compounds were applied to evaluate the inhibitory activities against KDM5B. Among them, 1-(4-methoxyphenyl)-N-(2-methyl-2-morpholinopropyl)-3-phenyl-1H-pyrazole-4-carboxamide (compound **27ab**) performed good inhibitory activity against KDM5B (IC_{50} = 0.0244 μM) and there was more than 382 folds increase in inhibitory activity compared to hit compound **5**. Further cellular study also indicated that compound **27ab** can stabilize KDM5B and induce the accumulation of H3K4me2/3 in gastric cancer cell line MKN45, which suggests that compound **27ab** is a potent and cellular active KDM5B inhibitor. Further biological study also indicated that compound **27ab** can inhibit MKN45 cell proliferation, colony formation and wound healing. Our finding gives a novel structure for the discovery of KDM5B inhibitor and compound **27ab** can be further developed and optimized as a chemical tool by targeting KDM5B, also, targeting KDM5B may be a new therapeutic strategy for gastric cancer treatment.

4. Materials and Methods

4.1. Chemistry

4.1.1. Materials

All the reagents and solvents used in the chemical synthesis were obtained from commercial sources and were used without further purification. ^{1}H NMR and ^{13}C NMR spectra data were obtained on Bruker AVANCE □ 400 M spectrometer (Bruker Instruments, Inc.), Chemical shifts (δ) were reported in parts per million (ppm) relative to tetramethylsilane (TMS) and *J* values were reported in Hertz. High

resolution mass spectra (HRMS) were recorded on a Waters Micromass Q-T of Micromass spectrometer by electrospray ionization (ESI) (Water, Milford, MA) and HPLC-Mass spectra were recorded on a Waters QDA. The NMR spectra data of compounds was provided in Supporting Information. All the chemistry reactions were monitored by thin layer chromatography (TLC) on silica gel. Column chromatography was carried out at medium pressure using silica gel (200-300 mesh) purchased from Qingdao Haiyang Chemical Co. Ltd. China. 1-Hydroxybenzo -triazole (HOBT), Phosphorus Oxychloride and 1-(3-Dimethyl -aminopropyl)-3-ethylcarbodiimide Hydrochloride (EDCI) were purchased from Beijing Yinuokai Science and Technology Ltd. China. Compound **5** was purchased from Enamine (product ID: Z647268608).

4.1.2. General procedure for preparation of the final compounds.

Procedure for preparation of compounds 13a-b, 14a-b

Substituted ketones (**6,** 5 mmol) was dissolved in ethanol (25 mL), then tert-butyl hydrazinecarboxylate (**7**, 5.5 mmol) and CH_3COOH (0.5 mmol) were sequentially added. The solution was heated under reflux for 4 hours, monitoring the progress of the reaction by TLC. After the reaction was completed, solvents were removed under vacuum. The residue was dissolved in DCM (5 mL) and CF_3COOH (7.5 mmol) were added, the solution was kept stirring under rt for 0.5h, after completion of the reaction, solvents were removed under vacuum, the remaining solid **8a-b** was used in the next step without further purification. DMF (3 mL) was slowly added phosphorus oxychloride (1 mL) under ice bath, stirring for 1 h to get Vilsmeier-Haack Reagent.

Then adding the **8a-b** (5 mmol) to the solution, stirring at room temperature for 30 min, then transferring to 80 □ for 4 h. After the reaction was over, the resulting mixture was slowly poured into ice-cold water, a saturated solution of sodium bicarbonate was added to neutralize the mixture, extracted with ethyl acetate. The organic phase was dried over Na_2SO_4, filtered and the solvent was evaporated under reduced pressure to afford crude product **9a-b**. To a stirring suspension of **9a-b** (5 mmol) in 10 mL of Dioxane/water (4:1), were added of KOH (6 mmol) and potassium permanganate (6 mmol). The mixture was stirred at room temperature for 3 h. Then slowly adding Hydrogen peroxide, MnO_2 was filtered. The dioxane in the filtrate were removed under reduced pressure and added water (10 mL), the solution was acidified to pH 1-2 with concentrated HCl, and the crude product was purified by column chromatography on silica gel to afford compounds **10a-b**. To a solution of **10a-b** (2 mmol) in dichloromethane (5 ml), EDCI (2.4 mmol) and HOBT (2.4 mmol) were added and the reaction mixture was stirred for 20 mins. To the reaction mixture compound **12** (2 mmol) was added and stirred overnight at room temperature. The reaction was diluted with water (30 mL) and extracted with DCM (2×30mL), the organic layers were combined, dried over $MgSO_4$, filtered, and evaporated under reduced pressure. The product **13a-b** was purified by column chromatography (EtOAc/hexane 3/1). Compounds **14a-b** were prepared through similar procedure as used for the synthesis of compound **13a-b** except **10a-b** were replaced by **11a-b**.

Procedure for preparation of compounds 27a-ac.

To the solution of ethanol (40 mL) was added substituted ketones (**6a,** 10 mmol) and phenylhydrazines (**15a**, 10 mmol) and CH_3COOH (11 mmol) were sequentially added. The solution was heated under reflux for 6-8 hours, monitoring the progress of the reaction by TLC. After the reaction was completed, solvents were removed under vacuum and the residue was diluted with water (25 mL) and filtered. The filter cake was washed repeatedly with a small amount of ethyl acetate, the remaining solid compound **16** was used in the next step without further purification. The mixture of DMF (3 mL) and phosphorus oxychloride (1 mL) was stirred for 1 h under ice bath, to get Vilsmeier-Haack Reagent. Then adding the compound **16** (5 mmol) to the solution, stirring at rt for 30 min, then transferring to 80 ° C for 4 h. After the reaction was over, the resulting mixture was slowly poured into ice-cold water, a saturated solution of sodium bicarbonate was added to neutralize the mixture, obtained solid **17** precipitate was filtered. To a stirred suspension of **17** (5 mmol) in 10 mL of Dioxane/water (4:1), were added of KOH (6 mmol) and potassium permanganate (6 mmol). The mixture was stirred at room temperature for 3 h. Then slowly adding Hydrogen peroxide, filter out the MnO_2 in the system. The dioxane in the filtrate were removed under reduced pressure and added water (10 mL), the solution was acidified to pH 1-2 with concentrated HCl, and the resulting precipitate was filtered to get compounds **18a**. Compounds **18b-r** were prepared through similar procedure as used for the synthesis of compound **18a** and some of them require column chromatography to purify.

The mixture of morpholine (**21**, 50 mmol), trimethylsilanecarbonitrile (**22,** 60 mmol**)** and acetone (**19**, 100mmol) or cyclohexanone (**20,** 100mmol) in alcohol (20mL) was

reflux for 5h and monitored by TLC. After completion of the reaction, the mixture was concentrated under reduced pressure. The residue was diluted with ethyl acetate and extracted with water. The organic phase was dried over Na_2SO_4, filtering and the solvent was evaporated under reduced pressure to afford crude product compound **23** and **25** respectively, which was used in the next step without further purification. Then compound **23** or **25** was dissolved in THF (8mL) at 0□, following the addition of $LiAlH_4$ (2eq). The reaction mixture was stirring for 6h under ice bath. After completion of the reaction, the mixture was added saturated ammonium chloride solution and 25% sodium hydroxide in aqueous solution (1: 1), and filtering, the crude product was purified by column chromatography on silica gel to afford compounds **24** and **26**, respectively. To a solution of **18a-r** (2 mmol) in dichloromethane (5 ml), EDCI (2.4 mmol) and HOBT (2.4 mmol) were added and the reaction mixture was stirred for 20 minutes. To the reaction mixture compound **24** or **26** or different substituted amino groups (2 mmol, shown in the Scheme 3) was added and stirred at room temperature for 12 h. The reaction was diluted with water (30 mL) and extracted with DCM (2×30mL), the organic layers were combined, dried over $MgSO_4$, filtered, and evaporated under reduced pressure. The product **27a-ac** was purified by column chromatography by using EtOAc/hexane. The reaction yield varies between 30-89% depending on the amine of the reactants.

Procedure for preparation of compounds 33a-b

To the solution of ethanol (40 mL) was added benzaldehyde (**28,** 10 mmol) and substituted phenylhydrazines (**15j or 15o**, 10 mmol) and CH_3COOH (11 mmol) were

sequentially added. The solution was heated under reflux for 6-8 hours, monitoring the progress of the reaction by TLC. After the reaction is complete, solvents were removed under vacuum and the residue was diluted with water (25 mL) and filtered. The filter cake was washed repeatedly with a small amount of ethyl acetate, the remaining solid compounds **29a-b** were used in the next step without further purification. To the solution of MeCN (5ml) was added compounds 2**9a-b** (5 mmol), thanolamine (15 mmol) and followed by the addition of iodine (I_2, 20 mol %) and tert-butyl hydroperoxide (TBHP, 70% aq. 5 mmol). The formed slurry was stirred at 90° C for 4 h, and monitored by (TLC). After cooling to rt and 20 mL water was added to the mixture, then extracted by EtOAc for 3 times (30mL×3). The extract was washed with 10% $Na_2S_2O_3$ solution(w/w), dried over anhydrous Na_2SO_4 and the solvent was removed in vacuo to provide a crude product compounds **31a-b**, which was purified by column chromatography on silica gel (PE/EA = 2/1).

Treatment of compounds **31a-b** (5mmol) with DMP (Dess-Martin periodinane,) in DCM (10 mL) at 0 □, then remove ice-bath, the solution was stirring under room temperature for 3h, monitoring the progress of the reaction by TLC. After the reaction is complete, and the residue was diluted with water (25 mL), then extracted by EtOAc for 3 times (20mL×3). The extract was washed with 10% $Na_2S_2O_3$ solution(w/w), dried over anhydrous Na_2SO_4 and the solvent was removed in vacuo to provide a crude product compounds **32a-b**, which were used in the next step without further purification.

To the solution of THF (10 mL) was added compounds **32a-b** (5 mmol) and compound **24** (5 mmol), then potassium tert-Butoxide (0.2eq) was sequentially added, then the solution was stirring under room temperature for 3h, monitoring the progress of the reaction by TLC. After the reaction is complete, solvents were removed under vacuum to provide a crude product compounds **33a-b**, which was purified by column chromatography on silica gel (PE/EA = 3/1).

4.1.3. 3-methyl-N-(2-morpholinoethyl)-1H-pyrazole-4-carboxamide (13a)

White solid, yield 70%, Mp: 107.3-107.9°C. ^{1}H NMR (400 MHz, $CDCl_3$) δ 13.09, (s, 1H), 7.88 (s, 1H), 6.34 (s, 1H), 3.57-3.55 (m, 4H), 3.37-3.32 (m, 2H), 2.45-2.39 (m, 6H), 2.25 (s, 3H). ^{13}C NMR (100.13 MHz, $CDCl_3$) δ 161.84, 146.85, 139.64, 103.80, 66.15, 57.29, 53.17, 35.32, 10.28. MS (ESI) found: m/z 239.16 $[M+H]^+$. HR-MS (ESI): Calcd. $C_{11}H_{18}N_4O_2$, $[M+H]^+$ m/z: 239.1508, found: 239.1519

4.1.4. N-(2-morpholinoethyl)-3-phenyl-1H-pyrazole-4-carboxamide (13b)

White solid, yield 89%, Mp: 100.1-100.3 °C. ^{1}H NMR (400 MHz, $CDCl_3$) δ 13.15, (s, 1H), 7.84 (s, 1H), 7.73-7.71 (m, 2H), 7.41-7.39 (m, 3H), 3.56 (s, 4H), 3.33 (s, 4H), 2.50-2.45 (m, 4H). ^{13}C NMR (100.13 MHz, $CDCl_3$) δ 163.12, 128.42, 127.98, 114.69, 65.90, 57.16, 53.02, 35.65. MS (ESI) found: m/z 301.20 $[M+H]^+$. HR-MS (ESI): Calcd. $C_{16}H_{20}N_4O_2$, $[M+H]^+$ m/z: 301.1665, found: 301.1658.

4.1.5. 5-methyl-N-(2-morpholinoethyl) nicotinamide (14a)

White solid, yield 85%, Mp: 139.3-142.5°C. ^{1}H NMR (400 MHz, $CDCl_3$) δ 8.98-8.95 (t, 1H), 8.88 (s, 1H), 8.65 (s, 1H), 8.12 (s, 1H), 4.02 (s, 2H), 3.69-3.64 (m, 4H), 3.57(s, 2H), 3.35-3.32(m, 2H), 3.15 (s, 2H), 2.39(s, 3H). ^{13}C NMR (100.13 MHz, $CDCl_3$) δ 165.18, 158.43, 158.08, 151.29, 144.78, 136.37, 63.23, 55.11, 51.22, 33.75, 17.72. MS (ESI) found: m/z 250.34 $[M+H]^+$. HR-MS (ESI): Calcd. $C_{13}H_{19}N_3O_2$, $[M+H]^+$ m/z: 250.1477, found:250.1449.

4.1.6. N-(2-morpholinoethyl)-5-phenylnicotinamide (14b)

White solid, yield 69%, Mp: 151.3-156.5°C. ^{1}H NMR (400 MHz, $CDCl_3$) δ 9.61 (s, 1H), 9.12 (s, 1H), 9.07 (s, 1H), 8.56 (s, 1H), 7.83-7.81 (d, *J* = 8 Hz, 2H), 7.59-7.57 (m, 2H), 7.52-7.48 (m, 1H), 4.04-4.01(m, 2H), 3.73-3.67 (m, 4H), 3.59-3.56(m, 2H), 3.37(s, 2H), 3.19(s, 2H). ^{13}C NMR (100.13 MHz, $CDCl_3$) δ 165.04, 149.13, 146.57, 135.86, 133.71, 129.71, 129.28, 128.80, 127.08, 63.26, 55.12, 51.28, 33.82. MS (ESI) found: m/z 312.29 $[M+H]^+$. HR-MS (ESI): Calcd. $C_{18}H_{21}N_3O_2$, $[M+H]^+$ m/z: 312.1712, found: 312.1708.

4.1.7. N-(2-morpholinoethyl)-1, 3-diphenyl-1H-pyrazole-4-carboxamide (27a)

White solid, yield 82%, Mp: 161.6-162.5°C. ^{1}H NMR (400 MHz, $CDCl_3$) δ 8.51 (s, 1H), 7.73 (dd, *J* = 20.2, 7.3 Hz, 4H), 7.48 (d, *J* = 6.9 Hz, 5H), 7.34 (t, *J* = 7.2 Hz, 1H), 6.27 (s, 1H), 3.51 – 3.37 (m, 6H), 2.37 (t, *J* = 5.6 Hz, 2H), 2.25 (s, 4H). ^{13}C NMR (100.13 MHz, $CDCl_3$) δ 162.62, 150.90, 139.40, 132.45, 131.01, 129.47, 129.13, 128.80, 127.30, 119.41, 118.30, 66.72, 56.58, 53.04, 35.65. MS (ESI): m/z 377.2 $[M+H]^+$. HR-MS (ESI) calcd. $C_{22}H_{24}N_4O_2$, $[M+H]^+$ m/z: 377.1977, found: 377.1976.

4.1.8. N-(2-morpholinoethyl)-1-phenyl-3-(thiophen-2-yl)-1H-pyrazole-4 -carboxamide (27b)

White solid, yield 43%, Mp: 132.2-133.1°C. ^{1}H NMR (400 MHz, $CDCl_3$) δ 8.5 (s, 1H), 7.75-7.73 (d, *J* = 8.0 Hz, 2H), 7.59-7.58 (d, *J* = 3.2 Hz, 1H), 7.49-7.43 (m, 3H), 7.36-7.32 (t, *J* = 8 Hz, 1H), 7.15-7.12 (dd, 1H), 6.75(s, 1H), 3.64-3.62 (m, 4H), 3.54-3.50 (m, 2H), 2.56-2.53 (m, 2H), 2.45(m, 4H). ^{13}C NMR (100.13 MHz, $CDCl_3$) δ 162.456, 144.798, 139.173, 133.764, 130.825, 129.577, 128.282, 127.496, 127.409, 127.283, 119.392, 118.098, 66.553, 56.860, 53.151, 35.547. MS (ESI): m/z 383.26 $[M+H]^+$. HR-MS (ESI) calcd. $C_{20}H_{22}N_4O_2S$, $[M+H]^+$ m/z: 383.1542, found: 383.1535.

4.1.9. N-(2-morpholinoethyl)-1-phenyl-3-(pyridin-4-yl)-1H-pyrazole-4 -carboxamide (27c)

White solid, yield 62%, Mp: 169.7-170.4°C. ^{1}H NMR (400 MHz, $CDCl_3$) δ 8.73-8.71 (dd, *J* = 4.4, 1.6Hz, 2H), 8.51(s, 1H), 7.76-7.75 (m, 4H), 7.52-7.48 (t, *J* = 8.4 Hz, 2H), 7.40-7.38 (t, *J* = 7.6 Hz, 1H), 7.36-7.32 (t, *J* = 7.6Hz, 1H), 6.50 (s, 1H), 3.59(s, 4H), 3.55-3.50 (m, 2H), 2.55 (m, 2H), 2.43 (m, 4H). ^{13}C NMR (100.13 MHz, $CDCl_3$) δ 162.43, 150.05, 148.53, 140.21, 139.19, 130.58, 129.64, 127.69, 123.39, 119.50, 118.59, 66.44, 56.81, 53.14, 35.52. MS (ESI): m/z 378.32 $[M+H]^+$. HR-MS (ESI) calcd. $C_{21}H_{23}N_5O_2$, $[M+H]^+$ m/z: 378.1930, found: 378.1921.

4.1.10. 3-(4-chlorophenyl)-N-(2-morpholinoethyl)-1-phenyl-1H-pyrazole-4 -carboxamide (27d)

White solid, yield 82%, Mp: 163.6-164.0°C. ^{1}H NMR (400 MHz, $CDCl_3$) δ 8.47 (s, 1H), 7.71 (dd, *J* = 23.5, 8.0 Hz, 4H), 7.48 (m, 4H), 7.35 (t, *J* = 7.3 Hz, 1H), 6.25 (s, 1H), 3.50 (s, 4H), 3.46-3.39 (m, 2H), 2.41 (t, *J* = 5.6 Hz, 2H), 2.29 (s, 4H). ^{13}C NMR (100.13 MHz, $CDCl_3$) δ 162.48, 149.79, 139.29, 135.23, 131.12, 130.59, 129.63, 128.94, 127.46, 119.42, 118.31, 66.73, 56.54, 53.10, 35.55. MS (ESI): m/z 411.2 $[M+H]^+$. HR-MS (ESI) calcd. $C_{22}H_{23}ClN_4O_2$, $[M+H]^+$ m/z: Mass: 411.1588, found: 411.1583.

4.1.11. 3-(4-methoxyphenyl)-N-(2-morpholinoethyl)-1-phenyl-1H-pyrazole-4-carboxamide (27e)

White solid, yield 70%, Mp: 150.0-150.2°C. ^{1}H NMR (400 MHz, $CDCl_3$) δ 8.49 (s, 1H), 7.76-7.74 (d, *J* = 8.0 Hz, 2H), 7.64-7.61 (d, *J* = 8.8 Hz, 2H), 7.49-7.45 (t, *J* = 8 Hz, 2H), 7.35-7.31 (t, *J* = 7.2 Hz, 1H), 7.02-6.99 (d, *J* = 8.8 Hz, 2H), 6.33 (s, 1H), 3.86 (s, 3H), 3.47 – 3.44 (m, 4H), 3.44-3.39 (m, 2H), 2.39-2.37 (m, 2H), 2.28-2.26 (m, 4H). ^{13}C NMR (100.13 MHz, $CDCl_3$) δ 162.73, 160.30, 150.77, 139.41, 130.90, 130.69, 129.54, 127.18, 124.59, 119.33, 118.09, 114.20, 66.69, 56.61, 55.32, 53.01. MS (ESI): m/z 407.33 $[M+H]^+$. HR-MS (ESI) calcd. $C_{23}H_{26}N_4O_3$, $[M+H]^+$ m/z: Mass:407.2083, found: 407.2077.

4.1.12. N-(2-morpholinoethyl)-1, 3-di-p-tolyl-1H-pyrazole-4-carboxamide (27f)

Solid, yield 85%, Mp: 128.1-129.5°C. ^{1}H NMR (400 MHz, $CDCl_3$) δ 8.52 (s, 1H), 7.76-7.74 (d, *J* = 8.0 Hz, 2H), 7.63-7.61 (d, *J* = 8 Hz, 2H), 7.48-7.44 (t, *J* = 8 Hz, 2H), 7.34-7.30 (m, 3H), 6.40 (s, 1H), 3.49-3.42 (m, 6H), 2.74-2.68 (m, 2H), 2.43-2.40 (m, 2H), 2.30-2.93 (m, 4H), 1.29-1.26 (t, *J* = 7.6 Hz, 3H). ^{13}C NMR (100.13 MHz, $CDCl_3$) δ 162.77, 151.08, 145.22, 139.41, 130.88, 129.70, 129.53, 129.30, 128.28, 127.18, 118.07, 66.57, 56.64, 53.02, 35.56, 31.58, 28.69, 15.32. MS (ESI): m/z 405.34 $[M+H]^+$. HR-MS (ESI) calcd. $C_{24}H_{28}N_4O_2$, $[M+H]^+$ m/z: Mass: 405.2291, found: 405.2282.

4.1.13. N-(2-morpholinoethyl)-1-phenyl-3-(o-tolyl)-1H-pyrazole-4-carboxamide (27g)

Solid, yield 69%, Mp: 130.8-131.4°C. ^{1}H NMR (400 MHz, $CDCl_3$) δ 8.60 (s, 1H), 7.77-7.75 (d, *J* = 8.0 Hz, 2H), 7.49-7.44 (m, 2H), 7.43-7.33 (m, 5H), 6.00 (s, 1H), 3.53(s, 4H), 3.37-3.31 (m, 2H), 2.29 (s, 3H), 2.28-2.26 (m, 5H). ^{13}C NMR (100.13 MHz, $CDCl_3$) δ 162.42, 150.38, 139.39, 137.91, 131.92, 130.74, 130.69, 130.53, 129.58, 129.55, 127.24, 126.28, 118.93, 66.59, 56.85, 53.09, 35.60, 19.93. MS (ESI): m/z 391.32 $[M+H]^+$. HR-MS (ESI) calcd. $C_{23}H_{26}N_4O_2$, $[M+H]^+$ m/z: Mass: 391.2134, found: 391.2128.

4.1.14. 3-(4-isopropylphenyl)-N-(2-morpholinoethyl)-1-phenyl-1H-pyrazole-4-carboxamide (27h)

Solid, yield 69%, Mp: 159.2-161.3°C. ^{1}H NMR (400 MHz, $CDCl_3$) δ 8.49 (s, 1H), 7.76-7.74 (d, *J* = 8.0 Hz, 2H), 7.65-7.63 (d, *J* = 8.0 Hz, 2H), 7.49-7.45 (t, *J* = 8.0 Hz, 2H), 7.36-7.27 (m, 3H), 6.34 (s, 1H), 3.47-3.42(m, 6H), 3.00-2.94 (m, 1H), 2.39-2.38 (m, 2H), 2.27 (s, 4H), 1.29-1.28 (d, *J* = 4.0 Hz, 6H). ^{13}C NMR (100.13 MHz, $CDCl_3$) δ 162.75, 150.95, 149.86, 139.40, 130.88, 129.80, 129.53, 129.24, 128.79, 127.18, 126.92, 126.64, 119.31, 118.13, 66.81, 56.55, 53.34, 53.02, 35.72, 33.97, 23.88. MS (ESI): m/z 419.38 $[M+H]^+$. HR-MS (ESI) calcd. $C_{25}H_{30}N_4O_2$, $[M+H]^+$ m/z: Mass: 419.2447, found: 419.2441.

4.1.15. 1-(4-chlorophenyl)-N-(2-morpholinoethyl)-3-phenyl-1H-pyrazole-4-carboxamide (27i)

Solid, yield 69%, Mp: 164.9-165.1°C. ^{1}H NMR (400 MHz, $CDCl_3$) δ 8.48 (s, 1H), 7.72-7.69 (m, 4H), 7.51-7.43 (m, 5H), 6.29 (s, 1H), 3.46 (m, 4H), 3.43-3.41(m, 2H), 2.39-2.36 (m, 2H), 2.26 (s, 4H). ^{13}C NMR (100.13 MHz, $CDCl_3$) δ 162.39, 151.14, 137.89, 132.85, 132.19, 130.93, 129.68, 129.31, 129.25, 128.82, 120.46, 118.63, 66.66, 56.55, 53.01, 35.61. MS (ESI): m/z 411.28 $[M+H]^+$. HR-MS (ESI) calcd. $C_{22}H_{23}ClN_4O_2$, $[M+H]^+$ m/z: Mass: 411.1588, found: 411.1582.

4.1.16. N-(2-morpholinoethyl)-3-phenyl-1-(p-tolyl)-1H-pyrazole-4-carboxamide (27j)

Light yellow solid, yield 81%, Mp: 144.6-144.7°C. ^{1}H NMR (400 MHz, $CDCl_3$) δ 8.46 (s, 1H), 7.70 (d, *J* = 7.9, 1.5 Hz, 2H), 7.63 (d, *J* = 8.4 Hz, 2H), 7.53-7.43 (m, 3H), 7.27 (t, *J* = 4.0 Hz, 2H), 6.27 (s, 1H), 3.52-3.37 (m, 6H), 2.42-2.35 (m, 5H), 2.26 (d, *J* = 4.2 Hz, 4H). ^{13}C NMR (100.13 MHz, DMSO) δ 162.66, 150.29, 136.83, 136.29, 132.39, 130.02, 129.74, 128.37, 127.83, 118.50, 117.79, 66.14, 57.29, 53.22, 36.04, 20.45. MS (ESI): m/z 391.2 $[M+H]^+$. HR-MS (ESI) calcd. $C_{23}H_{26}N_4O_2$, $[M+H]^+$ m/z: Mass: 391.2134,found: 391.2135.

4.1.17. N-(2-morpholinoethyl)-3-phenyl-1-(m-tolyl)-1H-pyrazole-4-carboxamide (27k)

Solid, yield 68%, Mp: 128.5-130.2°C. ^{1}H NMR (400 MHz, $CDCl_3$) δ 8.167 (s, 1H), 7.71-7.69 (d, *J* = 6.8 Hz, 2H), 7.49-7.45(m, 3H), 7.40-7.38 (m, 1H), 7.35-7.26(m, 3H), 6.29 (s, 1H), 3.47-3.41(m, 6H), 2.40-2.37(t, *J* = 6.0Hz, 2H), 2.34(s, 3H), 2.28-2.26(m, 3H). ^{13}C NMR (100.13 MHz, $CDCl_3$) δ 162.83, 150.31, 139.17, 134.90, 133.60, 132.51, 131.46, 129.39, 128.98, 128.73, 126.77, 126.04, 117.08, 66.74, 56.62, 53.05, 35.63, 18.19. MS (ESI): m/z 391.33 $[M+H]^+$. HR-MS (ESI) calcd. $C_{23}H_{26}N_4O_2$, $[M+H]^+$ m/z: Mass: 391.2134, found: 391.2425.

4.1.18. N-(2-morpholinoethyl)-3-phenyl-1-(o-tolyl)-1H-pyrazole-4-carboxamide (27l)

Solid, yield 79%, Mp: 133.3-133.9°C. ^{1}H NMR (400 MHz, $CDCl_3$) δ 8.51 (s, 1H), 7.72-7.70 (d, *J* = 6.8 Hz, 2H), 7.61(s, 1H), 7.53-7.45 (m, 4H), 7.37-7.33 (t, *J* = 8.0 Hz, 1H), 6.35 (s, 1H), 3.48(s, 4H), 3.46-3.42(m, 2H), 2.42(s, 3H), 2.41-2.39 (m, 2H), 2.29 (s, 4H). ^{13}C NMR (100.13 MHz, $CDCl_3$) δ 162.69, 150.90, 139.73, 139.33, 132.49, 131.01, 129.38, 129.34, 129.08, 128.76, 128.08, 120.18, 116.41, 66.57, 56.66, 53.02, 35.54, 21.46. MS (ESI): m/z 391.31 $[M+H]^+$. HR-MS (ESI) calcd. $C_{23}H_{26}N_4O_2$, $[M+H]^+$ m/z: Mass: 391.2134, found: 391.2123.

4.1.19. 1-(4-ethylphenyl)-N-(2-morpholinoethyl)-3-phenyl-1H-pyrazole-4-carboxamide (27m)

Solid, yield 68%, Mp: 119.9-120.1°C. ^{1}H NMR (400 MHz, $CDCl_3$) δ 8.46 (s, 1H), 7.71-7.69 (d, *J* = 6.4 Hz, 2H), 7.66-7.64(d, *J* = 8.4 Hz, 2H), 7.50-7.44 (m, 3H), 7.30-7.28(d, *J* = 8.4 Hz, 2H), 6.27 (s, 1H), 3.46(s, 4H), 3.44-3.39(m, 2H), 2.72-2.66(q, 2H), 2.38-2.35(m, 2H), 2.40 (s, 4H), 1.28-1.24(t, *J* = 7.6Hz, 3H). ^{13}C NMR (100.13 MHz, $CDCl_3$) δ 162.69, 150.67, 143.59, 137.29, 135.52, 130.92, 129.38, 129.05, 128.90, 128.77, 129.44, 118.00, 66.71, 56.58, 53.02, 35.61, 28.37, 15.51. MS (ESI): m/z 405.35 $[M+H]^+$. HR-MS (ESI) calcd. $C_{24}H_{28}N_4O_2$, $[M+H]^+$ m/z: Mass: 405.2291, found: 405.2281.

4.1.20. 1-(4-isopropylphenyl)-N-(2-morpholinoethyl)-3-phenyl-1H-pyrazole-4-carboxamide (27n)

Solid, yield 58%, Mp: 120.2-120.8°C. ^{1}H NMR (400 MHz, $CDCl_3$) δ 8.47 (s, 1H), 7.71-7.65 (m, 4H), 7.50-7.47(m, 2H), 7.33-7.31(d, *J* = 8.2Hz, 2H), 6.28 (s, 1H), 3.47(s, 4H), 3.44-3.42(m, 2H), 2.99-2.92(m, 1H), 2.39-2.36(m, 2H), 2.26(s, 4H), 1.28-1.27(d, *J* = 6.8Hz, 6H). ^{13}C NMR (100.13 MHz, $CDCl_3$) δ 162.73, 150.69, 148.25, 137.35, 132.55, 130.93, 129.39, 129.11, 129.04, 128.76, 125.72, 119.49, 119.16, 117.97, 66.68, 56.61, 53.03, 35.60, 33.73, 31.82, 23.93. MS (ESI): m/z

419.36 $[M+H]^+$. HR-MS (ESI) calcd. $C_{25}H_{30}N_4O_2$, $[M+H]^+$ m/z: Mass: 419.2447, found:419.2437.

4.1.21. 1-(4-methoxyphenyl)-N-(2-morpholinoethyl)-3-phenyl-1H-pyrazole-4-carboxamide (27o)

Solid, yield 58%, Mp: 167.5-168.3°C. ^{1}H NMR (400 MHz, $CDCl_3$) δ 8.40 (s, 1H), 7.70-7.64(m, 4H), 7.50-7.44(m, 3H), 6.99-6.97 (d, *J* = 9.2Hz, 2H), 6.27 (s, 1H), 3.85(s, 3H), 3.47(s, 4H), 3.44-3.40(m, 2H), 2.39-2.36(m, 2H), 2.26(s, 4H). ^{13}C NMR (100.13 MHz, $CDCl_3$) δ 162.73, 158.86, 150.58, 133.08, 132.56, 130.99, 129.39, 128.77, 121.07, 117.86, 114.65, 66.69, 56.61, 53.61, 35.59. MS (ESI): m/z 407.32 $[M+H]^+$. HR-MS (ESI) calcd. $C_{23}H_{26}N_4O_3$, $[M+H]^+$ m/z: Mass: 407.2083, found: 407.2085.

4.1.22. N-(2-(diisopropylamino) ethyl)-1, 3-diphenyl-1H-pyrazole-4-carboxamide (27p)

Yellow solid, yield 44%, Mp: 197.2-198.5°C.Mp: 132.5°C. ^{1}H NMR (400 MHz, $CDCl_3$) δ 8.77 (s, 1H), 7.85-7.75 (m, 4H), 7.44 (ddd, *J* = 11.1, 8.6, 5.4 Hz, 5H), 7.32 (t, *J* = 7.4 Hz, 1H), 3.54 (s, 2H), 3.18 (s, 2H), 2.84 (d, *J* = 32.2 Hz, 2H), 1.10 (s, 12H). ^{13}C NMR (100.13 MHz, $CDCl_3$) δ 163.14, 139.37, 132.45, 130.34, 129.53, 129.23, 128.78, 128.40, 127.14, 119.32, 51.62, 45.39, 38.04, 29.69, 19.35. MS (ESI): m/z 391.2 $[M+H]^+$. HR-MS (ESI) calcd. $C_{24}H_{30}N_4O$, $[M+H]^+$ m/z: Mass: 391.2498, found: 391.2497.

4.1.23. 1, 3-diphenyl-N-(prop-2-yn-1-yl)-1H-pyrazole-4-carboxamide (27q)

White solid, yield 87%, Mp: 186.1.6-186.9°C. ^{1}H NMR (400 MHz, $CDCl_3$) δ 8.51 (s, 1H), 7.75 (d, *J* = 7.7 Hz, 2H), 7.71 (dd, *J* = 7.8, 1.6 Hz, 2H), 7.54-7.44 (m, 5H), 7.35 (t, *J* = 7.4 Hz, 1H), 5.89 (s, 1H), 4.18-4.03 (m, 2H), 2.18 (t, *J* = 2.5 Hz, 1H). ^{13}C NMR (100.13 MHz, $CDCl_3$) δ 162.28, 150.94, 139.28, 131.95, 131.21, 129.59, 129.36, 129.25, 129.01, 127.42, 119.44, 117.43, 79.12, 71.54, 29.10. MS (ESI): m/z 302.1

$[M+H]^+$. HR-MS (ESI) calcd. $C_{19}H_{15}N_3O$, $[M+Na]^+$ m/z: Mass: 324.1113, found: 324.1112.

4.1.24. N-(2-methyl-2-(4-phenylpiperazin-1-yl) propyl)-1, 3-diphenyl-1H-pyraz -ole-4-carboxamide (27r)

Light yellow solid, yield52 %, Mp: 174.7-176.0°C. ^{1}H NMR (400 MHz, $CDCl_3$) δ 8.52 (s, 1H), 7.75 (d, *J* = 7.7 Hz, 2H), 7.70-7.63 (m, 2H), 7.51-7.37 (m, 5H), 7.33 (t, *J* = 7.4 Hz, 1H), 7.27-7.21 (m, 2H), 6.86 (t, *J* = 8.6 Hz, 3H), 6.42 (s, 1H), 3.31 (d, *J* = 4.4 Hz, 2H), 2.82 (d, *J* = 19.0 Hz, 4H), 2.56-2.38 (m, 4H), 0.98 (s, 6H). ^{13}C NMR (100.13 MHz, $CDCl_3$) δ 162.90, 151.24, 150.85, 139.39, 132.56, 131.13, 129.54, 129.47, 129.26, 129.05, 128.99, 127.23, 119.66, 119.37, 118.39, 115.96, 55.21, 49.53, 47.51, 44.93, 21.38. MS (ESI): m/z 480.3 $[M+H]^+$. HR-MS (ESI) calcd. $C_{30}H_{33}N_5O$, $[M+H]^+$ m/z: Mass: 480.2763, found: 480.2764

4.1.25. N-((1-morpholinocyclohexyl) methyl)-1, 3-diphenyl-1H-pyrazole-4-carboxamide (27s)

White solid, yield 75%, Mp: 164.2-165.0°C. ^{1}H NMR (400 MHz, $CDCl_3$) δ 9.29 (s, 1H), 8.97 (s, 1H), 8.48 (s, 1H), 7.92-7.90 (d, *J* = 8 Hz, 2H), 7.82-7.80 (d, *J* = 8 Hz, 2H), 7.60-7.57 (m, 2H), 7.44-7.40 (m, 4H), 4.02 (s, 2H), 3.77 (s, 4H), 3.28 (s, 2H), 2.06-2.04 (m, 2H), 1.74-1.54 (m, 7H), 1.24-1.14(m, 1H). ^{13}C NMR (100.13 MHz, $CDCl_3$) δ 164.36, 151.26, 138.91, 132.16, 130.62, 129.71, 128.37, 128.05, 127.18, 118.80, 116.89, 68.71, 63.93, 46.17, 37.26, 28.48, 24.18, 21.82. MS (ESI) found: m/z 445.47 $[M+H]^+$. HR-MS (ESI) calcd. $C_{27}H_{32}N_4O_2$, $[M+H]^+$ m/z: Mass: 445.2604, found: 445.2597.

4.1.26. (1, 3-diphenyl-1H-pyrazol-4-yl) (4-(2-(pyrrolidin-1-yl) ethyl) piperazin-1-yl) methanone (27t)

Yellow solid, yield 34%, Mp: 81.9-82.7°C. ^{1}H NMR (400 MHz, $CDCl_3$) δ 8.14 (s, 1H), 7.75 (d, *J* = 7.4 Hz, 2H), 7.71 (d, 2H), 7.47 (t, *J* = 7.9 Hz, 2H), 7.41 (t, *J* = 7.2 Hz, 2H), 7.37 (dd, *J* = 6.5, 3.8 Hz, 1H), 7.32 (d, *J* = 7.4 Hz, 1H), 3.77 (s, 2H), 3.25 (s,

2H), 3.06 (dd, *J* = 18.6, 11.2 Hz, 4H), 2.97 (t, *J* = 6.1 Hz, 2H), 2.58 (t, *J* = 6.2 Hz, 2H), 2.47 (s, 2H), 2.01 (d, *J* = 24.7 Hz, 6H). ^{13}C NMR (100.13 MHz, $CDCl_3$) δ 164.51, 150.10, 139.47, 132.22, 129.58, 128.79, 128.72, 128.25, 127.58, 127.15, 119.27, 116.64, 54.59, 54.16, 52.52, 23.13. MS (ESI): m/z 430.3 $[M+H]^+$. HR-MS (ESI) calcd. $C_{26}H_{31}N_5O$, $[M+H]^+$ m/z: Mass: 430.2607,found: 430.2609.

4.1.27. (1-(4-methoxyphenyl)-3-phenyl-1H-pyrazol-4-yl) (4-(2-(pyrrolidin-1-yl) ethyl) piperazin-1-yl) methanone (27u)

Yellow oil, yield 26%. ^{1}H NMR (400 MHz, $CDCl_3$) δ 8.11 (s, 1H), 7.73 (d, *J* = 9.9 Hz, 2H), 7.65 (d, *J* = 5.7 Hz, 2H), 7.48 (t, *J* = 7.9 Hz, 2H), 7.32 (t, *J* = 15.2, 7.9 Hz, 1H), 6.95 (d, *J* = 8.8 Hz, 2H), 3.85 (s, 3H), 3.82-3.68 (m, 2H), 3.38-3.03 (m, 6H), 2.98 (t, *J* = 5.9 Hz, 2H), 2.73 (t, *J* = 6.2 Hz, 2H), 2.49 (s, 2H), 2.01 (d, *J* = 34.9 Hz, 6H). ^{13}C NMR (100.13 MHz, $CDCl_3$) δ 164.59, 160.06, 149.91, 139.51, 129.55, 128.87, 128.19, 127.00, 124.85, 119.21, 116.28, 114.18, 55.40, 54.32, 53.48, 52.57, 52.09, 23.15. MS (ESI): m/z 460.3 $[M+H]^+$. HR-MS (ESI) calcd. $C_{27}H_{33}N_5O_2$, $[M+H]^+$ m/z: Mass: 460.2712, found: 460.2713.

4.1.28. (3-phenyl-1-(p-tolyl)-1H-pyrazol-4-yl) (4-(2-(pyrrolidin-1-yl) ethyl) piperazin-1-yl) methanone (27v)

Yellow solid, yield 35%, Mp: 67.9-74.9°C. ^{1}H NMR (400 MHz, $CDCl_3$) δ 8.11 (s, 1H), 7.74 (d, *J* = 7.9 Hz, 2H), 7.60 (d, *J* = 7.9 Hz, 2H), 7.48 (t, *J* = 7.8 Hz, 2H), 7.33 (t, *J* = 7.3 Hz, 1H), 7.23 (d, *J* = 7.9 Hz, 2H), 3.78 (s, 2H), 3.21 (s, 2H), 3.07 (m, 4H), 2.89 (s, 2H), 2.66 (t, *J* = 6.2 Hz, 2H), 2.49 (s, 2H), 2.39 (s, 3H), 1.99 (s, 6H). ^{13}C NMR (100.13 MHz, $CDCl_3$) δ 164.56, 150.22, 139.56, 138.61, 129.55, 129.44, 128.28, 127.49, 127.04, 119.28, 116.64, 54.39, 52.64, 23.27, 21.36. MS (ESI): m/z 444.3 $[M+H]^+$. HR-MS (ESI) calcd. $C_{27}H_{33}N_5O$, $[M+H]^+$ m/z: Mass: 444.2763, found: 444.2762.

4.1.29. (1, 3-di-p-tolyl-1H-pyrazol-4-yl) (4-(2-(pyrrolidin-1-yl) ethyl) piperazin-1-yl) methanone (27w)

Yellow solid, yield 33%, Mp: 91.9-93.7°C. ^{1}H NMR (400 MHz, $CDCl_3$) δ 8.07 (s, 1H), 7.60 (dd, *J* = 11.7, 8.3 Hz, 4H), 7.25 (s, 2H), 7.21 (d, *J* = 7.9 Hz, 2H), 3.76 (s, 2H), 3.45 (s, 2H), 3.23 (s, 2H), 3.04-2.91 (m, 4H), 2.89 (t, *J* = 6.2 Hz, 2H), 2.56 (t, *J* = 6.4 Hz, 2H), 2.44 (d, *J* = 24.1 Hz, 2H), 2.38 (d, *J* = 4.7 Hz, 6H), 2.01 (s, 2H), 1.94 (s, 4H). ^{13}C NMR (100.13 MHz, $CDCl_3$) δ 164.68, 149.91, 138.49, 137.29, 136.94, 130.05, 129.42, 128.12, 127.40, 119.19, 116.22, 54.62, 52.76, 23.17, 21.32, 20.96. MS (ESI): m/z 458.3 $[M+H]^+$. HR-MS (ESI) calcd. $C_{28}H_{35}N_5O$, $[M+H]^+$ m/z: Mass: 458.2920, found: 458.2919.

4.1.30. Methyl 3-(3-phenyl-1-(p-tolyl)-1H-pyrazole-4-carboxamido) propanoate (27x)

White solid, yield 79%, Mp: 139.6-140.0°C. ^{1}H NMR (400 MHz, $CDCl_3$) δ 8.43 (s, 1H), 7.67 (dd, *J* = 7.5, 1.8 Hz, 2H), 7.62 (d, *J* = 8.4 Hz, 2H), 7.51-7.44 (m, 3H), 7.27 (s, 1H), 7.25 (s, 1H), 6.15 (s, 1H), 3.60 (s, 3H), 3.59-3.53 (m, 2H), 2.52 (t, *J* = 6.1 Hz, 2H), 2.39 (s, 3H). ^{13}C NMR (100.13 MHz, $CDCl_3$) δ 172.37, 162.75, 150.73, 137.25, 137.13, 132.24, 130.75, 130.05, 129.18, 129.07, 128.84, 119.36, 117.77, 51.69, 34.82, 33.85, 20.97. MS (ESI): m/z 364.2 $[M+H]^+$. HR-MS (ESI) calcd. $C_{21}H_{21}N_3O_3$, $[M+Na]^+$ m/z: Mass: 386.1481, found: 386.1483.

4.1.31. 3-phenyl-N, 1-di-p-tolyl-1H-pyrazole-4-carboxamide (27y)

White solid, yield 80%, Mp: 154.6-154.9°C. ^{1}H NMR (400 MHz, DMSO) δ 10.11 (s, 1H), 9.02 (s, 1H), 7.84 (t, *J* = 8.3 Hz, 4H), 7.58 (d, *J* = 8.2 Hz, 2H), 7.43 (t, *J* = 7.1 Hz, 2H), 7.38 (t, *J* = 7.9 Hz, 3H), 7.15 (d, *J* = 8.2 Hz, 2H), 2.37 (s, 3H), 2.27 (s, 3H). ^{13}C NMR (100.13 MHz, DMSO) δ 161.35, 150.71, 136.81, 136.65, 136.40, 132.37, 132.31, 130.15, 130.07, 129.05, 128.23, 128.12, 128.09, 119.70, 118.53, 117.85, 20.46. MS (ESI): m/z 368.2 $[M+H]^+$. HR-MS (ESI) calcd. $C_{24}H_{21}N_3O$, $[M+H]^+$ m/z: Mass: 368.1763, found: 368.1764.

4.1.32. N-(2-methyl-2-morpholinopropyl)-3-phenyl-1-(p-tolyl)-1H-pyrazole-4 -carboxamide (27z)

White solid, yield 65%, Mp: 184.7-186.6°C. ^{1}H NMR (400 MHz, $CDCl_3$) δ8.48 (s, 1H), 7.71 (d, *J* = 6.8 Hz, 2H), 7.63 (d, *J* = 8.4 Hz, 2H), 7.53-7.44 (m, 3H), 7.27 (d, *J* = 4.0 Hz, 2H), 6.38 (s, 1H), 3.30 (s, 4H), 3.25 (d, *J* = 4.4 Hz, 2H), 2.39 (s, 3H), 2.31-2.22 (m, 4H), 0.93 (s, 6H). ^{13}C NMR (100.13 MHz, $CDCl_3$) δ 162.94, 150.58, 137.20, 137.14, 132.67, 131.12, 130.06, 129.52, 129.33, 129.13, 128.90, 119.38, 119.32, 118.07, 67.28, 55.26, 47.08, 45.35, 21.09, 20.98. MS (ESI): m/z 419.2 $[M+H]^+$. HR-MS (ESI) calcd. $C_{25}H_{30}N_4O_2$, $[M+H]^+$ m/z: Mass: 419.2447,found: 419.2448.

4.1.33. 1-(4-chlorophenyl)-N-(2-methyl-2-morpholinopropyl)-3-phenyl-1H-pyrazole-4-carboxamide (27aa)

White solid, yield 79%, Mp: 207.5-208.9°C. ^{1}H NMR (400 MHz, $CDCl_3$) δ 8.50 (s, 1H), 7.71 (d, *J* = 7.1, 4.9 Hz, 4H), 7.61-7.35 (m, 6H), 6.38 (s, 1H), 3.30 (s, 4H), 3.26 (s, 2H), 2.27 (s, 4H), 0.93 (s, 6H). ^{13}C NMR (100.13 MHz, $CDCl_3$) δ 162.64, 151.07, 137.91, 132.85, 132.36, 131.15, 129.68, 129.40, 128.96, 120.46, 118.73, 67.28, 55.25, 47.11, 45.37, 21.08. MS (ESI): m/z 439.1$[M+H]^+$. HR-MS (ESI) calcd. $C_{24}H_{27}ClN_4O_2$, $[M+H]^+$ m/z: Mass: 439.1901 found: 439.1903.

4.1.34. 1-(4-methoxyphenyl)-N-(2-methyl-2-morpholinopropyl)-3-phenyl-1H-pyrazole-4-carboxamide (27ab)

Solid, yield 85%, Mp: 169.1-171.4°C. ^{1}H NMR (400 MHz, $CDCl_3$) δ 8.42 (s, 1H), 7.71-7.69(d, *J* = 7.2Hz, 2H), 7.67-7.65(d, *J* = 9.2Hz, 2H), 7.52-7.43 (m, 3H), 6.99-6.97(d, *J* = 8.8Hz, 2H), 6.37(s, 1H), 3.85(s, 3H), 3.31(s, 4H), 3.26-3.25(m, 2H), 2.27(m, 4H), 0.94(s, 4H). ^{13}C NMR (100.13 MHz, $CDCl_3$) δ 162.97, 158.83, 150.48, 133.08, 132.70, 131.17, 129.52, 129.10, 128.89, 121.04, 117.93, 114.63, 67.28, 55.60, 55.27, 347.07, 45.37. MS (ESI): m/z 435.34 $[M+H]^+$. HR-MS (ESI) calcd. C25H30N4O3, $[M+H]^+$ m/z: Mass: 435.2396 found: 435.2389.

4.1.35. 1-(2-methoxyphenyl)-N-(2-methyl-2-morpholinopropyl)-3-phenyl-1H-pyrazole-4-carboxamide (27ac)

Solid, yield 62%, Mp: 165.0-165.9°C. ^{1}H NMR (400 MHz, $CDCl_3$) δ 9.67 (s, 1H), 8.770(s, 1H), 8.49v(s, 1H), 7.79-7.79 (m, 2H), 7.71-7.69 (m, 1H), 7.47-7.38(m, 4H), 7.33-7.31(m, 1H), 7.15-7.11 (s, 1H), 4.03-4.00(m, 2H), 3.92(s, 3H), 3.84-3.78(m, 2H), 3.59-3.55(m, 4H), 3.20-3.17(m, 2H), 1.35 (s, 6H). ^{13}C NMR (100.13 MHz, $CDCl_3$) δ 163.80, 157.75, 151.23, 150.72, 134.50, 132.48, 129.19, 128.61, 128.21, 128.09, 127.80, 125.08, 120.91, 115.73, 112.98, 66.33, 63.55, 56.14, 46.43, 43.51, 20.11. MS: m/z 434.54 $[M+H]^+$ (ESI) found: 435.37. HR-MS (ESI) calcd. C25H30N4O3, $[M+H]^+$ m/z: Mass: 435.2396 found: 435.2390.

4.1.36. 1-(4-methoxyphenyl)-N-(2-methyl-2-morpholinopropyl)-3-phenyl-1H-1, 2, 4-triazole-5-carboxamide (33a)

Solid, yield 32%, Mp: 143.4-144.2°C. ^{1}H NMR (400 MHz, $CDCl_3$) δ 9.26-9.24 (t, 1H), 8.12-8.11(d, *J* = 6.8Hz, 2H), 7.56-7.53(m, 5H), 7.08-7.06 (d, *J* = 8.4Hz, 2H), 4.00(s, 2H), 3.84(s, 3H), 3.61(s, 4H), 3.18(s, 4H), 1.34(s, 6H). ^{13}C NMR (100.13 MHz, $CDCl_3$) δ 159.85, 159.61, 158.00, 147.85, 130.79, 129.88, 129.76, 128.90, 126.79, 126.10, 113.82, 66.41, 63.59, 55.52, 46.50, 43.49, 20.10. MS: m/z 435.53 $[M+H]^+$ (ESI) found: 436.34. HR-MS (ESI) calcd. $C_{24}H_{29}N_5O_3$, $[M+H]^+$ m/z: Mass: 436.2349 found: 436.2343.

4.1.37. N-(2-methyl-2-morpholinopropyl)-3-phenyl-1-(p-tolyl)-1H-1, 2, 4-triazole-5-carboxamide (33b)

Solid, yield 45%, Mp: 144.4-145.1°C. ^{1}H NMR (400 MHz, $CDCl_3$) δ 8.48 (s, 1H), 8.10-8.08(d, *J* = 8 Hz, 2H), 7.56-7.47(m, 5H), 7.34-7.32 (d, *J* = 8.4Hz, 2H), 3.59(s, 4H), 3.24-3.23(d, *J* = 4.0Hz, 3H), 2.39(s, 3H), 0.98(s, 6H). ^{13}C NMR (100.13 MHz, $CDCl_3$) δ 159.77, 157.06, 148.71, 138.76, 135.23, 129.84, 129.81, 129.23, 128.93, 125.96, 124.89, 67.03, 56.01, 45.82, 45.63, 20.97, 20.68. MS: m/z 419.53 $[M+H]^+$ (ESI) found: 420.36. HR-MS (ESI) calcd. $C_{24}H_{29}N_5O_2$, $[M+H]^+$ m/z: Mass: 420.2400 found: 420.2390.

4.2. KDM5B assay

KDM5B assay was performed in 384-well white plates (PerkinElmer, USA) as previously reported [41]. Demethylase buffer conditions for KDM5B recombinant (Active Motif, USA) were as follows: 10 μM α-KG, 100 μM ascorbate, 50 μM $(NH_4)_2Fe(SO_4)_2$, 50 mM HEPES (pH 7.5), 0.01% (v/v) Tween 20, and 0.1% (w/v) bovine serum albumin. For the experiment group, candidate compound was incubated with 4 nM KDM5B recombinant first, and then 64 nM biotin-H3K4me3, the substrate peptide, was added to the reaction system to have a 10 μL reaction system. After incubation, the value was read out with microplate reader (Envision, PerkinElmer, USA) in ALPHA model by adding Strep-Tactin ® donor beads (AlphaLISA , PerkinElmer, USA) and methyl-H3K4me1-2 antibody tagged acceptor beads (AlphaLISA, PerkinElmer, USA). Finally, data were normalized to the blank control and the IC50 was determined using GraphPad Prism 6 (Prism, USA).

4.3. Cell culture

The human gastric carcinoma cell line AGS, NCI-N87, MKN45, MGC-803, SGC-7901, HGC-27 and BGC-823 were supplied by the Cell Bank of Shanghai Institute of Cell Biology, Chinese Academy of Sciences. Cells were cultured in DMEM medium or RPMI-1640 medium. All media were supplemented with 10% FBS (BI, Israel). Cells were cultured in an incubator with 5% CO_2 at 37 °C and the medium was changed every 2 days.

4.4. Western blotting

Protein was extracted using RIPA buffer, and the western blotting was performed according to a standard method. Approximately 30μg of protein was electrophoresed on 10% SDS□PAGE gel and transferred to 0.2 μm nitrocellulose membranes (P/N66485, Pall, USA). The membranes were blocked with 5% milk dissolved in phosphate buffer saline (PBS) for 2 hours and then inculcated with indicated antibodies, including KDM5B (1:1000, Sigma, USA), histone 3 (1:5000, Abcam, USA), GAPDH (1:5000, Abcam, USA), H3K4me1 (1:1000, Abcam, USA), H3K4me2 (1:1000, Abcam, USA), H3K4me3 (1:1000, CST, USA), H3K9me2

(1:2000, Abcam, USA) , H3K9me3 (1:2000, CST, USA) , H3K27me2 (1:1000, Abcam, USA). GAPDH and histone 3 were used as loading control. The membranes were washed with PBST at room temperature and incubated with secondary antibody (Peroxidase-conjugated goat anti-rabbit Ig, ZB-2301, Zsbio, China; peroxidase-conjugated goat anti-mouse IgG, ZB-2305, Zsbio, China) for 2 hours at room temperature. Then, the membrane was washed with PBST at room temperature and visualized by enhanced chemiluminescence reagent (34096, thermo fisher, USA).

4.5. Cellular thermal shift assay

Cells (5×10^5) were treated with a compound or with DMSO for 1 h, washed with PBS three times, and dissolved in 50 μl PBS supplemented with a protease inhibitor cocktail, followed by heating at the indicated temperatures in a PCR instrument (Senso, Germany). Treated cells were then subjected to snap-freezing in liquid nitrogen and thawed on ice for 3 cycles. The protein levels of KDM5B in equal amounts of the supernatant were examined by western blotting assay. GAPDH was used as the control.

4.6. High content screening

MKN45 cells were seeded in plate and incubated for 24 h. After indicated treatment, cells were fixed with 4% paraformaldehyde and then washed three times with PBS (5 min/wash). After that, cells were permeabilized with 0.1% Triton X-100 for 20 min at room temperature. After blocking cells with 5% bovine serum albumin in PBS for 1 h at room temperature, then incubated cells with primary antibody at 4°C overnight. Finally, cells were incubated with an Alexa Fluor® 488 Rabbit Anti-Goat IgG (H+L) and cell nuclei were stained with Hoechst 33342 (5 μg/mL, Solarbio Life Sciences, Beijing, China) for 10 min. The immunofluorescence images were imaged and

quantified using high content screening system (ArrayScan XTI, Thermo Fisher Scientific, USA).

4.7. Cell proliferation

Cells were plated in 96-well plates (3×10^3 cells per well) and treated with drugs as indicated. After incubation, cell proliferation was determined using MTS assay (Promega, USA) according to the manufacture's protocol.

4.8. Colony formation assay

1000 MKN45 cells were seeded in 6-well plates and treated. After the incubation, medium was replaced and cells were cultured for another 10 days. Finally, cells were fixed with cold methanol and subjected to the staining using crystal violet (Beyotime Biotechnology, China), and photographed under a microscope (Nikon, Japan).

4.9. Wound healing assay

MKN45 cells were seeded into 6-well plate and grown to complete confluence after 24h. Then a 200μl pipette tip was used to make a straight scratch wound in the center of the plate, after which the plates were washed with PBS to strip the floating cells and the medium was changed to fresh medium with 2% fetal bovine serum and indicated compounds. The wound was photographed under a microscope (Nikon, Japan) at 0h, 6h, 12, 24h and 48h.

4.10 Statistical analysis

Pearson correlation coefficient was used to evaluate the correlationship between groups. Results were considered statistically significant at $P < 0.05$. $P < 0.01$ was considered highly significant. All analyses were carried out by using SPSS 21.0 software. In this study, the statistical analyses were performed with Student's *t* Test. $^*P < 0.05$, $^{**}P < 0.01$.

4.11 HTVS

The structure-based HTVS was applied to the Enamine database including 2 million drug-like organic molecules and our in-house compound library (approximate 500 compounds). The molecules were washed and processed and prepared the 3D conformation of small molecules by Energy Minimize using MOE platform (v201608). KDM5B protein structure was extracted from Protein Data Bank with code 5FYZ (PDB code: 5FYZ, Resolution: 1.75 Å) and we constructed pharmacophore with common characteristics based on the overlapping of active pockets of 29 resolved crystal structures of KDM5B. A pharmacophore guided docking-based VS was then performed and followed with an additional evaluation on the ADMET property. The top 300 hit compounds were identified with the highest binding score as well as desired ADMET properties. Finally, the structural diversity analysis was carried out based on molecular fingerprint algorithm calculation, and the top twelve hit compounds with stable binding to the target and potential high activity were selected manually for biological activity assay.

ASSOCIATED CONTENT

AUTHOR INFORMATION

Corresponding Authors

*Hong-Min Liu, e-mail: liuhm@zzu.edu.cn. Phone: 86-371-67781936.

*Yi-Chao Zheng, e-mail: yichaozheng@zzu.edu.cn.

*Li-Ying Ma, e-mail: maliying@zzu.edu.cn

Author Contributions

#These authors contributed equally to this work.

Notes

The authors declare no competing financial interest.

ACKNOWLEDGMENTS

This work was supported by National Natural Science Foundation of China (Project No. 81903447, No. 81602961, No. 81430085, No. 21372206, No. 81703328); National Key Research Program (No. 2018YFE0195100, No. 2016YFA0501800 and No. 2017YFD0501401); Science and Technology Innovation Talents of Henan Provincial Education Department (19IRTSTHN001). We thank Xiaoling Zhang (Zhengzhou University) for providing the computing resources for docking analysis.

References:

[1]. W.A. Flavahan, E. Gaskell,B.E. Bernstein, Epigenetic plasticity and the hallmarks of cancer, Science. 357 (2017) eaal2380.

[2]. M. Esteller, Cancer epigenomics: DNA methylomes and histone-modification maps, Nat. Rev. Genet. 8 (2007) 286-98.

[3]. A. Lujambio, S. Ropero, E. Ballestar, M.F. Fraga, C. Cerrato, F. Setien, S. Casado, A. Suarez-Gauthier, M. Sanchez-Cespedes, A. Git, I. Spiteri, P.P. Das, C. Caldas, E. Miska,M. Esteller, Genetic unmasking of an epigenetically silenced microRNA in human cancer cells, Cancer Res. 67 (2007) 1424-9.

[4]. M.F. Fraga, E. Ballestar, A. Villar-Garea, M. Boix-Chornet, J. Espada, G. Schotta, T. Bonaldi, C. Haydon, S. Ropero, K. Petrie, N.G. Iyer, A. Perez-Rosado, E. Calvo, J.A. Lopez, A. Cano, M.J. Calasanz, D. Colomer, M.A. Piris, N. Ahn, A. Imhof, C. Caldas, T. Jenuwein,M. Esteller, Loss of acetylation at Lys16 and trimethylation at Lys20 of histone H4 is a common hallmark of human cancer, Nat. Genet. 37 (2005) 391-400.

[5]. A. Roberti, A.F. Valdes, R. Torrecillas, M.F. Fraga,A.F. Fernandez, Epigenetics in cancer therapy and nanomedicine, Clin. Epigenetics. 11 (2019) 81.

[6]. N. Mosammaparast,Y. Shi, Reversal of histone methylation: biochemical and molecular mechanisms of histone demethylases, Annu. Rev. Biochem. 79 (2010) 155-79.

[7]. S.S. Ng, W.W. Yue, U. Oppermann,R.J. Klose, Dynamic protein methylation in chromatin biology, Cell. Mol. Life Sci. 66 (2009) 407-22.

[8]. C. Martin,Y. Zhang, The diverse functions of histone lysine methylation, Nat. Rev. Mol. Cell Biol. 6 (2005) 838-49.

[9]. Z. Zhao,A. Shilatifard, Epigenetic modifications of histones in cancer, Genome Biol. 20 (2019) 245.

[10]. T.E. McAllister, K.S. England, R.J. Hopkinson, P.E. Brennan, A. Kawamura,C.J. Schofield, Recent Progress in Histone Demethylase Inhibitors, J. Med. Chem. 59 (2016) 1308-29.

[11]. B. Lohse, J.L. Kristensen, L.H. Kristensen, K. Agger, K. Helin, M. Gajhede,R.P. Clausen, Inhibitors of histone demethylases, Bioorg Med Chem. 19 (2011) 3625-36.

[12]. D. Han, M. Huang, T. Wang, Z. Li, Y. Chen, C. Liu, Z. Lei,X. Chu, Lysine methylation of transcription factors in cancer, Cell Death Dis. 10 (2019) 290.

[13]. S.M. Kooistra,K. Helin, Molecular mechanisms and potential functions of histone

demethylases, Nat Rev Mol Cell Biol. 13 (2012) 297-311.

[14]. D. Rotili,A. Mai, Targeting Histone Demethylases: A New Avenue for the Fight against Cancer, Genes Cancer. 2 (2011) 663-79.

[15]. Y. Huang, S.N. Vasilatos, L. Boric, P.G. Shaw,N.E. Davidson, Inhibitors of histone demethylation and histone deacetylation cooperate in regulating gene expression and inhibiting growth in human breast cancer cells, Breast Cancer Res Treat. 131 (2012) 777-89.

[16]. S. Catchpole, B. Spencer-Dene, D. Hall, S. Santangelo, I. Rosewell, M. Guenatri, R. Beatson, A.G. Scibetta, J.M. Burchell,J. Taylor-Papadimitriou, PLU-1/JARID1B/KDM5B is required for embryonic survival and contributes to cell proliferation in the mammary gland and in ER+ breast cancer cells, Int. J. Oncol. 38 (2011) 1267-77.

[17]. I. Mocavini, S. Pippa, V. Licursi, P. Paci, D. Trisciuoglio, C. Mannironi, C. Presutti,R. Negri, JARID1B expression and its function in DNA damage repair are tightly regulated by miRNAs in breast cancer, Cancer Sci. 110 (2019) 1232-1243.

[18]. S. Pippa, C. Mannironi, V. Licursi, L. Bombardi, G. Colotti, E. Cundari, A. Mollica, A. Coluccia, V. Naccarato, G. La Regina, R. Silvestri,R. Negri, Small Molecule Inhibitors of KDM5 Histone Demethylases Increase the Radiosensitivity of Breast Cancer Cells Overexpressing JARID1B, Molecules. 24 (2019).

[19]. Y. Li, L. Chen, L. Feng, M. Zhu, Q. Shen, Y. Fang, X. Liu,X. Zhang, NEK2 promotes proliferation, migration and tumor growth of gastric cancer cells via regulating KDM5B/H3K4me3, Am. J. Cancer Res. 9 (2019) 2364-2378.

[20]. W. Xu, B. Zhou, X. Zhao, L. Zhu, J. Xu, Z. Jiang, D. Chen, Q. Wei, M. Han, L. Feng, S. Wang, X. Wang, J. Zhou,H. Jin, KDM5B demethylates H3K4 to recruit XRCC1 and promote chemoresistance, Int. J. Biol. Sci. 14 (2018) 1122-1132.

[21]. J. Bao, J.H. Zou, C.Y. Li,G.Q. Zheng, miR-194 inhibits gastric cancer cell proliferation and tumorigenesis by targeting KDM5B, Eur Rev Med Pharmacol Sci. 20 (2016) 4487-4493.

[22]. Z. Wang, F. Tang, G. Qi, S. Yuan, G. Zhang, B. Tang,S. He, KDM5B is overexpressed in gastric cancer and is required for gastric cancer cell proliferation and metastasis, Am. J. Cancer Res. 5 (2015) 87-100.

[23]. X. Wang, N. Oishi, T. Shimakami, T. Yamashita, M. Honda, S. Murakami,S. Kaneko, Hepatitis B virus X protein induces hepatic stem cell-like features in hepatocellular carcinoma by activating KDM5B, World J Gastroenterol. 23 (2017) 3252-3261.

[24]. M. Rao, N. Chinnasamy, J.A. Hong, Y. Zhang, M. Zhang, S. Xi, F. Liu, V.E. Marquez, R.A. Morgan,D.S. Schrump, Inhibition of histone lysine methylation enhances cancer-testis antigen expression in lung cancer cells: implications for adoptive immunotherapy of cancer, Cancer Res. 71 (2011) 4192-204.

[25]. X. Shen, Z. Zhuang, Y. Zhang, Z. Chen, L. Shen, W. Pu, L. Chen,Z. Xu, JARID1B modulates lung cancer cell proliferation and invasion by regulating p53 expression, Tumour Biol. 36 (2015) 7133-42.

[26]. Y.C. Zheng, J. Chang, L.C. Wang, H.M. Ren, J.R. Pang,H.M. Liu, Lysine demethylase 5B (KDM5B): A potential anti-cancer drug target, Eur. J. Med. Chem. 161 (2019) 131-140.

[27]. B. Xhabija,B.L. Kidder, KDM5B is a master regulator of the H3K4-methylome in stem cells, development and cancer, Semin. Cancer Biol. 57 (2019) 79-85.

[28]. A. Tumber, A. Nuzzi, E.S. Hookway, S.B. Hatch, S. Velupillai, C. Johansson, A. Kawamura, P. Savitsky, C. Yapp, A. Szykowska, N. Wu, C. Bountra, C. Strain-Damerell, N.A. Burgess-

Brown, G.F. Ruda, O. Fedorov, S. Munro, K.S. England, R.P. Nowak, C.J. Schofield, N.B. La Thangue, C. Pawlyn, F. Davies, G. Morgan, N. Athanasou, S. Müller, U. Oppermann,P.E. Brennan, Potent and Selective KDM5 Inhibitor Stops Cellular Demethylation of H3K4me3 at Transcription Start Sites and Proliferation of MM1S Myeloma Cells, Cell Chemical Biology. 24 (2017) 371-380.

[29]. C. Johansson, S. Velupillai, A. Tumber, A. Szykowska, E.S. Hookway, R.P. Nowak, C. Strain-Damerell, C. Gileadi, M. Philpott, N. Burgess-Brown, N. Wu, J. Kopec, A. Nuzzi, H. Steuber, U. Egner, V. Badock, S. Munro, N.B. LaThangue, S. Westaway, J. Brown, N. Athanasou, R. Prinjha, P.E. Brennan,U. Oppermann, Structural analysis of human KDM5B guides histone demethylase inhibitor development, Nat. Chem. Biol. 12 (2016) 539-45.

[30]. S.M. Westaway, A.G. Preston, M.D. Barker, F. Brown, J.A. Brown, M. Campbell, C.W. Chung, H. Diallo, C. Douault, G. Drewes, R. Eagle, L. Gordon, C. Haslam, T.G. Hayhow, P.G. Humphreys, G. Joberty, R. Katso, L. Kruidenier, M. Leveridge, J. Liddle, J. Mosley, M. Muelbaier, R. Randle, I. Rioja, A. Rueger, G.A. Seal, R.J. Sheppard, O. Singh, J. Taylor, P. Thomas, D. Thomson, D.M. Wilson, K. Lee,R.K. Prinjha, Cell Penetrant Inhibitors of the KDM4 and KDM5 Families of Histone Lysine Demethylases. 1. 3-Amino-4-pyridine Carboxylate Derivatives, J. Med. Chem. 59 (2016) 1357-69.

[31]. M. Vinogradova, V.S. Gehling, A. Gustafson, S. Arora, C.A. Tindell, C. Wilson, K.E. Williamson, G.D. Guler, P. Gangurde, W. Manieri, J. Busby, E.M. Flynn, F. Lan, H.J. Kim, S. Odate, A.G. Cochran, Y. Liu, M. Wongchenko, Y. Yang, T.K. Cheung, T.M. Maile, T. Lau, M. Costa, G.V. Hegde, E. Jackson, R. Pitti, D. Arnott, C. Bailey, S. Bellon, R.T. Cummings, B.K. Albrecht, J.C. Harmange, J.R. Kiefer, P. Trojer,M. Classon, An inhibitor of KDM5 demethylases reduces survival of drug-tolerant cancer cells, Nat. Chem. Biol. 12 (2016) 531-8.

[32]. B.K. Shoichet, Virtual screening of chemical libraries, Nature. 432 (2004) 862-5.

[33]. C. McInnes, Virtual screening strategies in drug discovery, Curr. Opin. Chem. Biol. 11 (2007) 494-502.

[34]. K.H. Bleicher, H. Böhm, K. Müller,A.I. Alanine, Hit and lead generation: beyond high-throughput screening, Nat. Rev. Drug Discov. 2 (2003) 369
EP.

[35]. R.V. Ganga, R.T. Srinivasa, N.V. Lakshma, B. Prasad, A.P. Reddy, A. Ravikumar, S. Taj,A. Kamal, Design, synthesis and biological evaluation of N-((1-benzyl-1H-1,2,3-triazol-4-yl)methyl)-1,3-diphenyl-1H-pyrazole-4-carboxamide s as CDK1/Cdc2 inhibitors, Eur. J. Med. Chem. 122 (2016) 164-177.

[36]. O. Prakash, K. Pannu,A. Kumar, Synthesis of some new 2-(3-aryl-1-phenyl-4-pyrazolyl)-benzoxazoles using hypervalent iodine mediated oxidative cyclization of Schiff's bases, Molecules. 11 (2006) 43-8.

[37]. M.A. Kira, M.O. Abdel-Rahman,K.Z. Gadalla, The vilsmeier-haack reaction - III Cyclization of hydrazones to pyrazoles, Tetrahedron Lett. 10 (1969) 109-110.

[38]. D.B. Dess,J.C. Martin, Readily accessible 12-I-5 oxidant for the conversion of primary and secondary alcohols to aldehydes and ketones, The Journal of Organic Chemistry. 48 (1983) 4155-4156.

[39]. J. Sayegh, J. Cao, M.R. Zou, A. Morales, L.P. Blair, M. Norcia, D. Hoyer, A.J. Tackett, J.S. Merkel,Q. Yan, Identification of small molecule inhibitors of Jumonji AT-rich interactive domain 1B (JARID1B) histone demethylase by a sensitive high throughput screen, J. Biol.

Chem. 288 (2013) 9408-17.

[40]. K. Debiec,J. Wydmanski, Chapter 8 - Gastric Cancer Metastasis, in Introduction to Cancer Metastasis, A. Ahmad, A. Ahmad Editors. 2017, Academic Press. p. 137-161.

[41]. J. Sayegh, J. Cao, M.R. Zou, A. Morales, L.P. Blair, M. Norcia, D. Hoyer, A.J. Tackett, J.S. Merkel,Q. Yan, Identification of small molecule inhibitors of Jumonji AT-rich interactive domain 1B (JARID1B) histone demethylase by a sensitive high throughput screen, J. Biol. Chem. 288 (2013) 9408-17.

Highlights:

1) Pyrazole derivatives were discovered as novel KDM5B inhibitors with the aid of high-throughput virtual screening and biochemical screening.

2) 35 compounds were synthesized and studied on their KDM5B inhibitory activities for SARs.

3) Compound **27ab** is a potent and cellular active KDM5B inhibitor that can inhibit MKN45 cell proliferation, colony formation and wound healing.

Declaration of interests

☒ The authors declare that they have no known competing financial interests or personal relationships that could have appeared to influence the work reported in this paper.

☐The authors declare the following financial interests/personal relationships which may be considered as potential competing interests: